OPEN ACCESS Freely available online

PLoS GENETICS

Roles of *brca2* (*fancd1*) in Oocyte Nuclear Architecture, Gametogenesis, Gonad Tumors, and Genome Stability in Zebrafish

Adriana Rodríguez-Marí[1], Catherine Wilson[1], Tom A. Titus[1], Cristian Cañestro[1¤], Ruth A. BreMiller[1], Yi-Lin Yan[1], Indrajit Nanda[2], Adam Johnston[3], John P. Kanki[3], Erin M. Gray[1], Xinjun He[1], Jan Spitsbergen[4], Detlev Schindler[2], John H. Postlethwait[1]*

1 Institute of Neuroscience, University of Oregon, Eugene, Oregon, United States of America, **2** Institute of Human Genetics, Biocenter, University of Würzburg, Würzburg, Germany, **3** Dana Farber Cancer Institute, Boston, Massachusetts, United States of America, **4** Marine and Freshwater Biomedical Sciences Center, Oregon State University, Corvallis, Oregon, United States of America

Abstract

Mild mutations in *BRCA2 (FANCD1)* cause Fanconi anemia (FA) when homozygous, while severe mutations cause common cancers including breast, ovarian, and prostate cancers when heterozygous. Here we report a zebrafish *brca2* insertional mutant that shares phenotypes with human patients and identifies a novel *brca2* function in oogenesis. Experiments showed that mutant embryos and mutant cells in culture experienced genome instability, as do cells in FA patients. In wild-type zebrafish, meiotic cells expressed *brca2*; and, unexpectedly, transcripts in oocytes localized asymmetrically to the animal pole. In juvenile *brca2* mutants, oocytes failed to progress through meiosis, leading to female-to-male sex reversal. Adult mutants became sterile males due to the meiotic arrest of spermatocytes, which then died by apoptosis, followed by neoplastic proliferation of gonad somatic cells that was similar to neoplasia observed in ageing *dead end* (*dnd*)-knockdown males, which lack germ cells. The construction of animals doubly mutant for *brca2* and the apoptotic gene *tp53* (*p53*) rescued *brca2*-dependent sex reversal. Double mutants developed oocytes and became sterile females that produced only aberrant embryos and showed elevated risk for invasive ovarian tumors. Oocytes in double-mutant females showed normal localization of *brca2* and *pou5f1* transcripts to the animal pole and *vasa* transcripts to the vegetal pole, but had a polarized rather than symmetrical nucleus with the distribution of nucleoli and chromosomes to opposite nuclear poles; this result revealed a novel role for Brca2 in establishing or maintaining oocyte nuclear architecture. Mutating *tp53* did not rescue the infertility phenotype in *brca2* mutant males, suggesting that *brca2* plays an essential role in zebrafish spermatogenesis. Overall, this work verified zebrafish as a model for the role of Brca2 in human disease and uncovered a novel function of Brca2 in vertebrate oocyte nuclear architecture.

Citation: Rodríguez-Marí A, Wilson C, Titus TA, Cañestro C, BreMiller RA, et al. (2011) Roles of *brca2* (*fancd1*) in Oocyte Nuclear Architecture, Gametogenesis, Gonad Tumors, and Genome Stability in Zebrafish. PLoS Genet 7(3): e1001357. doi:10.1371/journal.pgen.1001357

Editor: Mary C. Mullins, University of Pennsylvania School of Medicine, United States of America

Received August 3, 2010; **Accepted** February 28, 2011; **Published** March 31, 2011

Funding: Work was supported by grants 1R01GM085318, 1P01HL048546, and 2R01RR020833 from NIH to JHP; by a grant from the Schroeder-Kurth Fund to JHP; by grant BFU2010-14875 from the Ministerio de Ciencia e Innovación (MICINN) to CC; and by grants from the Fanconi Anemia Research Fund (http://www.fanconi.org/) to JPK and JHP. The funders had no role in study design, data collection and analysis, decision to publish, or preparation of the manuscript.

Competing Interests: The authors have declared that no competing interests exist.

* E-mail: jpostle@uoneuro.uoregon.edu

¤ Current address: Departament de Genètica, Universitat de Barcelona, Barcelona, Spain

Introduction

People who are heterozygous for strong mutations in the tumor suppressor gene *BRCA2*(*FANCD1*) have increased susceptibility to breast, ovarian, prostate, and pancreatic cancers [1-3]. Breast cancer risk for females heterozygous for germline mutations in *BRCA2* is nearly 60% by age 50 [4] and for ovarian cancer is 11% [5]. *BRCA2* is expressed in a broad range of mammalian tissues [6,7] and null activity alleles are embryonic lethal in mouse and humans but are viable in rats [8-11]. Biallelic inheritance of hypomorphic *BRCA2* mutations in the germline results in Fanconi anemia (FA), a disease characterized by catastrophic anemia, genome instability, characteristic morphological defects, and enormously elevated risk for leukemia (800 fold) and squamous cell carcinomas (2000 fold) [12-14]. The *BRCA2* subtype of Fanconi anemia represents complementation group D1 [15] and results in a severe form of the disease with nearly 100% incidence of leukemia and/or solid tumors by 5 years of age [16,17]. The role of BRCA2 in tumor suppression and maintenance of genomic integrity is associated with its function in error-free, homology-directed recombination (HDR) [18]. HDR helps repair DNA breaks associated with meiosis, and mouse mutants in *FA* genes have defects in meiotic cells [19]. Zebrafish *fancl* mutants experience female-to-male sex reversal due to the apoptotic loss of meiotic oocytes at the time of sex determination [20], consistent with the abnormal activation of the apoptotic pathway in the absence of Fanconi gene activity [21].

The involvement of *BRCA2* in HDR, ovarian cancer, hypogonadal phenotypes, and the expression of *Brca2* in mouse spermatocytes [22] converge to suggest a role for Brca2 in gonadogenesis. Homozygous *Brca2* knockout mice die as embryos [23], but transgenic mice

Author Summary

Women with one strong *BRCA2*(*FANCD1*) mutation have high risks of breast and ovarian cancer. People with two mild *BRCA2*(*FANCD1*) mutations develop Fanconi Anemia, which reduces DNA repair leading to genome instability, small gonads, infertility, and cancer. Humans and mice lacking *BRCA2* activity die before birth. We discovered that zebrafish *brca2* mutants show chromosome instability and small gonads, and they develop only as sterile adult males. Female-to-male sex reversal is due to oocyte death during sex determination. Normal animals expressed *brca2* in developing eggs and sperm that are repairing DNA breaks associated with genetic reshuffling. Normal developing eggs localized *brca2* RNA near the nucleus, suggesting a role in protecting rapidly dividing early embryonic cells. Sperm-forming cells died in adult mutant males. Inhibition of cell death rescued sex reversal, but not fertility. Rescued females developed invasive ovarian tumors and formed eggs with abnormal nuclear architecture. The novel role of Brca2 in organizing the vertebrate egg nucleus may provide new insights into the origin of ovarian cancer. These results validate zebrafish as a model for human *BRCA2*-related diseases and provide a tool for the identification of substances that can rescue zebrafish *brca2* mutants and thus become candidates for therapeutic molecules for human disease.

carrying a *BRCA2*-containing human BAC that expresses the human gene at high levels everywhere except the gonads survive as sterile males and females [24]. In contrast, rats bearing a premature stop codon survive, but show slow growth and sterility [10], reflecting conserved and lineage-specific roles of *brca2*.

To help understand the roles of Brca2 in vertebrates, we characterized zebrafish bearing an insertional mutation in *brca2*. We show here that comparative analysis of zebrafish *brca2* [25] identifies a few conserved, and hence putatively functional, coding regions and is expressed in proliferating somatic cells and in meiotic oocytes and spermatocytes. Surprisingly, *brca2* transcript is asymmetrically localized to the animal pole of the cytoplasm in developing wild-type oocytes. The insertional *brca2* null activity allele causes genome instability, slow growth of tissue culture cells, male sterility, testicular neoplasias, and female-to-male sex reversal that is rescued by mutation of the tumor suppressor gene *tp53*(*p53*). Male and female double mutants are sterile and develop testicular neoplasias and invasive ovarian tumors. Nuclear symmetries are strikingly altered in oocytes of double mutant females, revealing a novel role of Brca2 in establishing or maintaining the architecture of the vertebrate oocyte nucleus. This work reveals that this zebrafish *brca2* mutant is a model for unraveling gene functions as well as a valuable tool for small-molecule screens to help discover therapeutic compounds for human patients.

Results

Zebrafish *brca2* Shares with Human *BRCA2* Features of the Genome, Gene, and Protein

We isolated, cloned, and sequenced a zebrafish *brca2* cDNA (NM_001110394) and a BAC clone (AC149226). Because the zebrafish Brca2 protein shares only 21% identity with human BRCA2, we confirmed orthology by conserved syntenies [26]. Our meiotic mapping on the HS panel [27] showed that *brca2* lies on zebrafish chromosome 15 (*Dre*15, Figure 1A top), and sequence data at Ensembl (http://www.ensembl.org/Danio_rerio/Info/Index) showed that its genomic neighborhood contains 14 genes with conserved synteny to the orthologous region on human chromosome 13 (Hsa13, Figure 1A middle), as would be expected if zebrafish *brca2* and human *BRCA2* are orthologs. The absence of a second copy of *brca2* in the co-orthologous region in *Dre*10 (Figure 1A bottom) provides evidence that, like all 13 other zebrafish *fanc* genes [25,28], *brca2* evolved to single copy in the zebrafish lineage after the teleost genome duplication [27,29-31].

A comparison of our cDNA and BAC sequences revealed that zebrafish *brca2* has 26 exons (numbered 2–27 to follow human nomenclature; Figure 1B) like its tetrapod ortholog [7,32-34]. Despite low sequence identity (21%), zebrafish Brca2 conserves an N-terminal acidic transcriptional activation domain and a C-terminal DNA binding domain (DBD) [35-37] (Figure 1C). Exon-11, with 1,397 amino acid residues in zebrafish and 1,643 residues in human, is one of the longest vertebrate exons, 28 times larger than average [38]. Use of the stickleback *brca2* sequence (Figure S1) to help inform alignments showed that exon-11 of zebrafish *brca2* contains a central array of BRC repeats conserved in approximate number, relative position, and sequence identity to those in tetrapods [34] (Figure S2A). Phylogenetic analysis of BRC repeats revealed orthology between chicken and human repeats 1, 5, 7, and 8 (Figure 1D) but not a one-to-one orthology between zebrafish and tetrapod repeats, suggesting that some individual repeats may have evolved independently by tandem duplication and/or gene conversion. Despite differences in BRC repeat sequences, the correlation of hydrophobicity indexes among repeats revealed great structural similarity (Figure 1E). The DBDs of zebrafish and human Brca2 contain three oligonucleotide binding folds (OB1-3) and a helical domain (HD) [37] (Figure 1C and Figure S3). The mapping of human tumor-derived mutations to these conserved features [37] supports the hypothesis that they are critical for functionally similar molecular interactions across vertebrates.

brca2 Is Expressed in Meiotic Germ Cells

In zebrafish embryos, *brca2* has been shown to be expressed maternally and zygotically [25], and this is confirmed here by RT-PCR (Figure S4A) and histological sections that show broad expression that is elevated in rapidly proliferating cells in the embryonic and larval central nervous system, in the proliferating ventricle margins of adult brains, in the blood-forming kidney marrow, and in the proliferative intervillus region of the intestine [39] (Figure S4B-S4N). Germ line cells expressed *brca2* in both male and female gonads in transitional stages (Figure 2A, 2B), in immature gonads (Figure 2C, 2D), and in the mature gonads of adults (Figure 2E, 2F). Somatic cells of the zebrafish gonad either do not express *brca2*, or do so at a low level like mouse Sertoli cells [40].

Unexpectedly, in stage III and IV oocytes, *brca2* transcripts became asymmetrically distributed to a small peripheral patch of the ooplasm (Figure 2E). Comparison with the distribution of *pou5f1*(*oct4*) [41,42] revealed that *brca2* mRNA transcripts accumulated asymmetrically at the animal pole of the oocyte (Figure 2G, 2H). Expression of *brca2* was obvious in spermatocytes (sc, Figure 2F), but not in spermatids and sperm (sp, Figure 2F), as in mouse [40]. Expression of *brca2* in meiotic cells is consistent with a role in repairing DNA breaks associated with meiotic HDR. Furthermore, the accumulation of *brca2* transcript at the animal pole suggests a role of maternal message in provisioning embryos with Brca2 protein that could help effect DNA repair during the rapid cleavage divisions that occur before the initiation of zygotic transcription at the mid-blastula transition.

A Zebrafish *brca2* Null Allele Shows That *brca2* Is Required for Genome Stability

To understand *brca2* function, we studied a zebrafish line with the insertional mutation ZM_00057434, which disrupts *brca2* exon-11 in

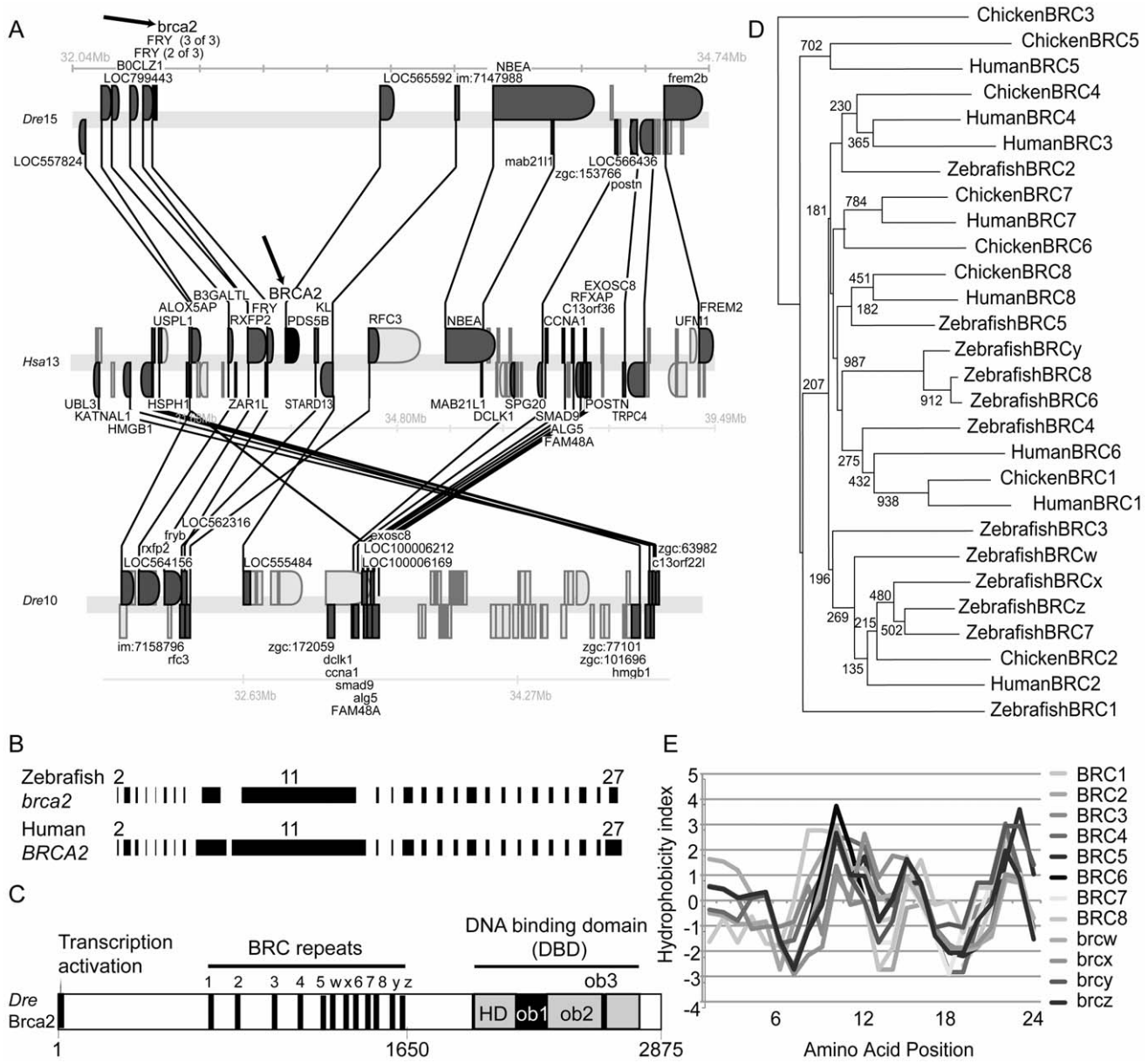

Figure 1. Zebrafish *brca2* genomics and Brca2 structure. (A) Syntenies conserved between human and zebrafish *brca2* chromosomes were examined using the Synteny database [26]. Synteny analysis shows that the portion of zebrafish linkage group 15 (*Dre*15) that contains *brca2* (arrow, top row) possesses many genes that are orthologous to, and in the same order as, genes in the portion of human chromosome 13 (*Hsa*13) that contains *BRCA2* (arrow, middle row). A portion of *Dre*10 is co-orthologous to the portion of *Hsa*13 that contains *BRCA2* but has no *brca2* gene (lower row). Genes represented above the line are transcribed to the right and those below to the left. Gene names are from Ensembl. Lines connect orthologs (dark gray). (B) Exons (black bars) in zebrafish *brca2* are similar in size to orthologous exons in human *BRCA2*, including the large exon-10 and the enormous exon-11. Introns not drawn to scale. (C) Zebrafish Brca2 protein shares domain structure with the human protein. Amino acid positions are listed below. (D) BRCA2 proteins were aligned and phylogenetic trees were inferred using ClustalW [90] and diagrammed with NJPlot [91]. Phylogenetic analysis of human, chicken, and zebrafish BRC repeats shows that individual BRCs are mostly not orthologous. A strongly supported clade grouped BRCy with zebrafish BRC 6 and 8, as expected if they arose by tandem duplication or experienced gene conversion. Numbers at nodes are bootstrap values for 1000 runs. (E) Comparison of amino acid hydrophobicities of aligned BRC repeats used the Kyte–Doolittle method [92]. Correlation of hydrophobicity indices among zebrafish BRC repeats shows that the physical properties of BRC repeats have been maintained despite residue evolution.
doi:10.1371/journal.pgen.1001357.g001

BRC repeat-z (Figure 1C, Figure 3A and 3B, Figure S2). Reverse transcriptase-PCR and sequence analysis detected no normal transcript in mutants, but instead identified two aberrant transcripts, one lacking the DBD and the other lacking all BRC repeats (Figure 3C–3G). Because Brca2 protein cannot function without either of these features [37], we conclude that ZM_00057434 is a null allele.

Genome instability is a cardinal characteristic of Fanconi anemia [43,44]. Cell cultures from fins of homozygous *brca2* zebrafish mutants and wild-type controls revealed normal karyotypes ($2n = 50$) with low levels of spontaneous breakage (Figure 3H). After treatment with 10 ng/ml of the DNA-damage agent MMC, however, mutant cells showed many chromosome

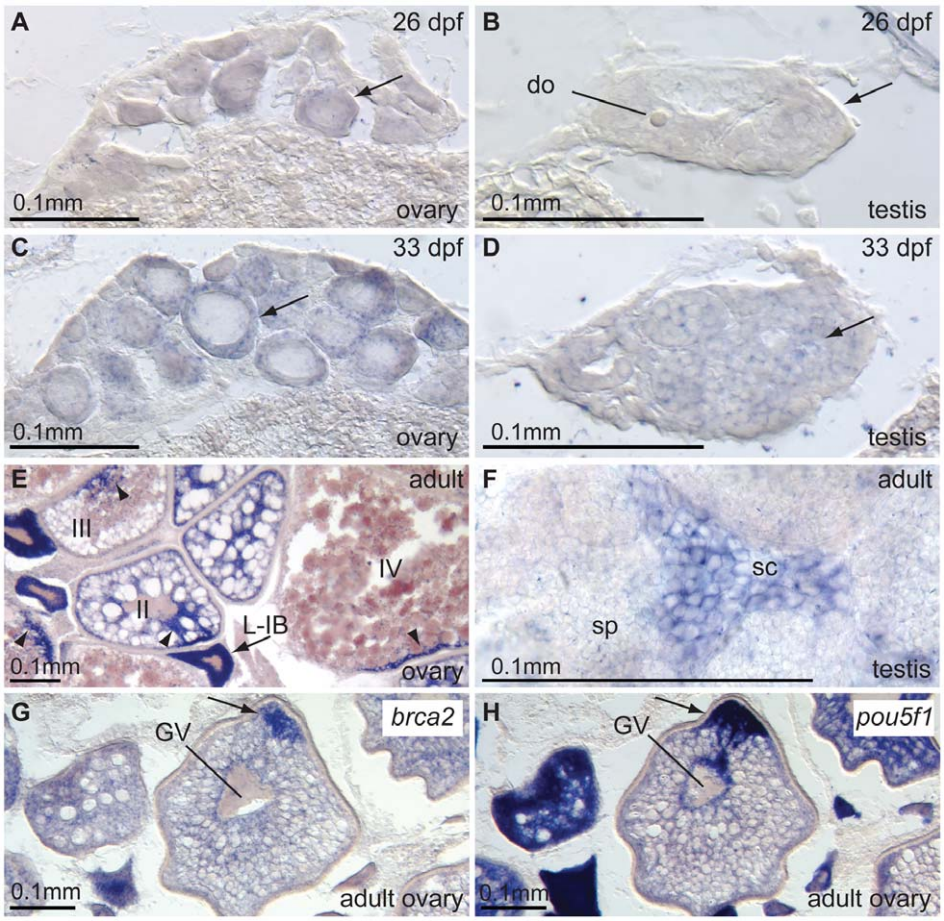

Figure 2. Expression of *brca2* in wild-type gonads. (A,B) 26dpf transitioning stage ovaries and testes, respectively, express *brca2* in the ooplasm of oocytes (arrow) and in male germ cells. (C,D) Expression of *brca2* increases in 33dpf immature ovaries and testis, respectively. Arrows indicate examples of *brca2*-expressing cells. (E) In wild-type ovaries, *brca2* transcript is highly expressed in the ooplasm of late stage IB oocytes (L-IB, arrow) and gradually becomes localized to a small portion of the ooplasm in stage III and IV oocytes (arrowheads). (F) Spermatocytes contain *brca2* transcript but spermatids and sperm do not. (G) Stage III-IV oocytes accumulate *brca2* transcript in a pole of the oocyte. (H) Comparison to the adjacent section probed for the animal pole marker *pou5f1*(*oct4*) reveals that brca2 transcript localizes to the animal pole in the same location as *pou5f1*(*oct4*) message (arrows in G and H). Abbreviations: II, III, IV, stages of oocyte development; L-IB, late stage IB oocyte (stages according to [49]); do, degenerating oocyte; GV, germinal vesicle; sc, spermatocyte; sp, sperm.
doi:10.1371/journal.pgen.1001357.g002

aberrations, including chromatid and chromosome breaks, radial reunion figures, and acentric chromosome fragments. Of 100 metaphases counted in mutant cells, 66 showed chromosome aberrations, including 32 that showed one or two anomalies, 23 with 3 or 4 abnormal chromosomes, and 11 with more than 5 aberrations (Figure 3I). In contrast, all 24 metaphases from wild-type cells treated with MMC were normal (Figure 3H). These results show that zebrafish cells require *brca2* activity to prevent chromosome aberrations.

To test genome stability in living animals, we crossed *brca2* heterozygotes, stained resulting embryos at 28hpf with acridine orange (AO, which fluoresces strongly when it intercalates into DNA with double-strand breaks [45]), scored the amount of AO staining in individual embryos, and genotyped embryos by PCR. Untreated mutants and wild-type controls had about the same amount of AO staining (Figure 3J, 3K). In contrast, after treatment with the DNA damage agent diepoxybutane (DEB) at 4hpf, mutants accumulated substantially more AO-positive cells than wild-type siblings (Figure 3L-3N). Thus, we conclude that Brca2 helps protect zebrafish embryos from DNA damage.

To learn the role of *brca2*(*fancd1*) in zebrafish somatic cells, we established tissue cultures from fin biopsies of *brca2* mutants and wild types and studied their growth rates. Mutant cultures showed significantly slower growth compared to wild-type cultures (Figure 3O, $p<0.001$ at day 5). Addition of MMC further delayed culture growth both for *brca2* mutants ($p<0.5$ vs. untreated) and for wild types, although delay in wild types was not statistically significant (Figure 3O). The poor growth of *brca2* mutant cultures was due to high rates of spontaneous apoptosis (15%, Figure 3P-3S), as evidenced by propidium iodide exclusion and anti-active Caspase-3 staining. In *brca2* mutants, addition of MMC increased the non-apoptotic cell death rate from 2.9% to 4.8% while the proportion of apoptotic cells remained essentially the same (15.0 and 14.1%, respectively, Figure 3P, 3Q). Untreated wild-type cultures revealed much less spontaneous apoptosis than mutant cultures (2% vs. 15%; Figure 3R) and showed just a small effect of MMC on the non-apoptotic cell death rate (2.0% untreated, 3.9% treated, Figure 3S). We conclude that mutant cultures grow more slowly than wild-type cultures due to high rates of spontaneous apoptosis.

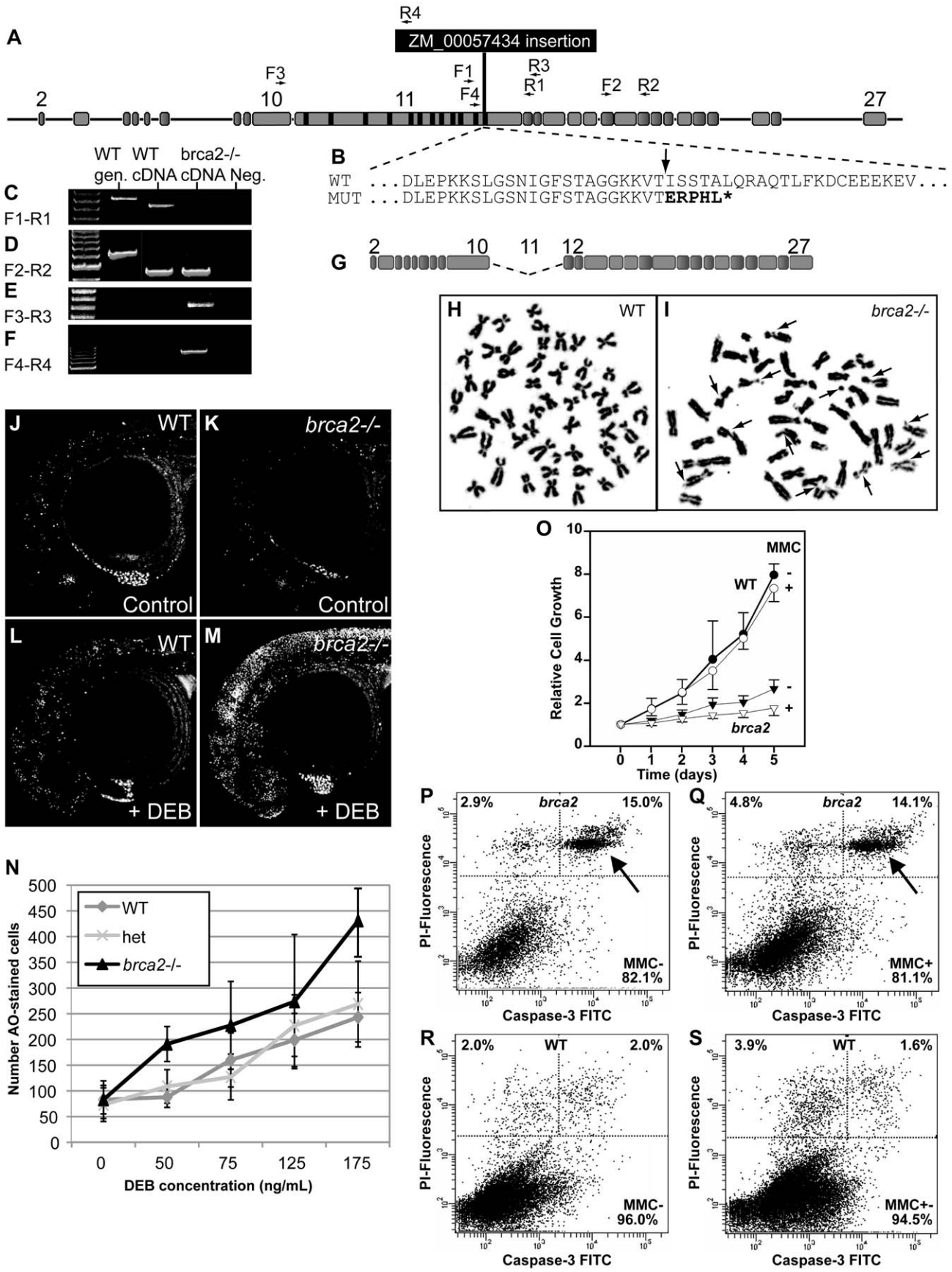
A
R4
ZM_00057434 insertion
F3
F1
R3
R1
F4
F2
R2
2
10
11
27
B
WT ...DLEPKKSLGSNIGFSTAGGKKVTISSTALQRAQTLFKDCEEEKEV...
MUT ...DLEPKKSLGSNIGFSTAGGKKVTERPHL*
WT gen.
WT cDNA
brca2-/- cDNA
Neg.
C
F1-R1
D
F2-R2
E
F3-R3
F
F4-R4
G
2
10
11
12
27
H
WT
I
brca2-/-
J
WT
Control
K
brca2-/-
Control
L
WT
+ DEB
M
brca2-/-
+ DEB
O
Relative Cell Growth
Time (days)
MMC
WT
brca2
N
Number AO-stained cells
DEB concentration (ng/mL)
WT
het
brca2-/-
P
2.9%
brca2
15.0%
MMC-
82.1%
PI-Fluorescence
Caspase-3 FITC
Q
4.8%
brca2
14.1%
MMC+
81.1%
PI-Fluorescence
Caspase-3 FITC
R
2.0%
WT
2.0%
MMC-
96.0%
PI-Fluorescence
Caspase-3 FITC
S
3.9%
WT
1.6%
MMC+-
94.5%
PI-Fluorescence
Caspase-3 FITC

Figure 3. A zebrafish *brca2* insertional mutant reveals a role for *brca2* in zebrafish genome stability and cell growth. (A) The ZM_00057434 insertion disrupts exon-11 of zebrafish *brca2* in the last BRC repeat. (B) The insertion (arrow) disrupts the wild-type (WT) sequence, leading to a mutant (MUT) sequence that contains five substituted amino acid residues encoded by the insert followed by a stop codon (*) that truncates the protein before the DNA binding domain, which is essential for Brca2 activity. (C) Amplification using primers F1 and R1 (see panel A and Table S1) produced a transcript from wild-type cDNA but none from homozygous mutant cDNA. (D) Amplification using primers F2 and R2 showed that transcripts including exon-18 occur in both wild types and mutants. (E) Amplification using primers F3 and R3 revealed that mutants, but not wild types, made transcripts that lack exon-11. (F) Amplification using primers F4 and R4 showed that mutants, but not wild types, made transcripts that include part of exon-11 and the insert. (G) The transcript amplified in panel F is predicted to make a transcript that lacks exon-11 but continues in-frame and makes a non-functional protein lacking all BRC repeats. (H) Most tissue culture cells established from the caudal fin of wild-type adults had a normal karyotype even after MMC treatment. (I) Most tissue culture cells established from the caudal fin of homozygous *brca2* mutant adults showed chromatid breaks after MMC treatments, including acentric fragments, and radial chromosomes (arrows). (J,K) Acridine orange (AO) treatment of wild types and *brca2* mutants not treated with DEB revealed about equal levels of cells staining with AO. (L,M) After DEB treatment, the number of AO-positive cells increased a small amount in 28hpf wild-type embryos but increased substantially in 28hpf *brca2* mutant embryos. (N) The number of AO-positive cells increased with DEB concentration in all three genotypes tested, but nearly twice as much in *brca2* mutant cells. (O-S) Growth, apoptosis and non-apoptotic cell death in cultured zebrafish fibroblasts. (O) Cell cultures established from *brca2* mutant caudal fins (*brca2*, triangles) grew slower than cultures established from wild types (circles), reaching only 33.5% of the control count after 5 days. The additional effect of 15 nM mitomycin C (MMC) on growth retardation was relatively low but more distinct in *brca2* mutant cultures than wild-type cultures (open triangles and open circles, respectively). The graph displays the mean and standard deviation of multiples of the seeded cell number from three independent experiments. (P-S) Apoptosis is mainly responsible for the growth deficit of *brca2* mutant cells. (P) Untreated *brca2* cultures showed spontaneous apoptosis of 15% of cells (upper right quadrant) and 2.9% of cells experienced non-apoptotic death (upper left quadrant). (Q) Exposure to 50 nM mitomycin C for 24 h increased the non-apoptotic cell death rate in *brca2* mutant cultures only to 4.8%, whereas the rate of apoptotic cells remained about the same (14.1%). (R) Wild-type cultures revealed just 2% spontaneous apoptosis (upper right quadrant) and 2% non-apoptotic cell death (upper left quadrant). (S) Exposure to 50 nM mitomycin C for 24 h increased the non-apoptotic cell death rate to 3.9% but left the rate of apoptotic cells unchanged (1.6%).
doi:10.1371/journal.pgen.1001357.g003

Lack of *brca2* Activity Causes Female-to-Male Sex Reversal

To test the viability of zebrafish *brca2* mutants, we mated heterozygotes, and among 414 adult offspring, 24.9% were homozygous wild types, 44.9% were heterozygotes, and 30.2% were homozygous mutants, a ratio indistinguishable from the expected 1:2:1 ratio (X^2 test, $p = 0.37$, $df = 2$). We conclude that zebrafish *brca2* mutants survive about as well as wild types, as in *Drosophila* [46]. In addition, zebrafish *brca2*(*fancd1*) mutants expressed genes for primitive and definitive hematopoiesis normally (Figure S5), providing no evidence for the early hematopoietic defects found in human FA patients.

Remarkably, however, all homozygous *brca2* mutants developed exclusively as males. A series of heterozygote in-crosses gave 199 wild-type homozygotes and heterozygotes, about half of which were females (50.2%±0.1% (sd)). In contrast, of the 61 homozygous mutants, none were female (X^2 test, $p = 0.00003$, $df = 2$). Genotypic ratios following Mendelian principles ruled out female-specific lethality; thus, we conclude that individuals that would otherwise have become females experienced female-to-male sex reversal. Homozygous *brca2* mutant males were sterile (the 35 males tested fertilized no eggs, with an average clutch size of 197 eggs tested per male), but wild-type sibling males were all fertile (the 28 males tested fertilized an average of 80% of the eggs per male with an average clutch size of 210 eggs tested per male). These data show that *brca2* plays a role in male fertility and is necessary for female development in otherwise wild-type fish.

Juvenile Gonads of *brca2* Mutants Lack Perinucleolar Oocytes and Sperm

To investigate the developmental basis of sex reversal in *brca2* mutants, we analyzed transitional and immature (but differentiated) gonads. All juvenile zebrafish, regardless their definitive sex, initially develop oocytes; in females, these oocytes continue to develop but in males, they disappear [47,48]. In our experiments, some wild types at 21dpf contained perinucleolar oocytes (early stage IB) and other wild types contained a few pyknotic cells and oocytes at earlier stages of development (early oocytes at stage IA (leptotene to pachytene) [49]) (Figure 4A, 4B). In contrast, all eight homozygous *brca2* mutants examined at 21dpf lacked perinucleolar oocytes and contained earlier stage oocytes and large numbers of pyknotic cells (Figure 4C). By 27dpf, wild types contained either ovaries or testes (Figure 4D, 4E). All eight *brca2* mutants analyzed, however, showed testis-like gonads that lacked perinucleolar oocytes but retained a few early oocytes and pyknotic cells (Figure 4F). At 32dpf, perinucleolar oocytes in wild-type animals reached late stage IB and entered diplotene, as indicated by the presence of lampbrush chromosomes (Figure 4G), while testes of wild-type males showed all stages of spermatogenesis including sperm (Figure 4H). In contrast, all eight *brca2* mutants analyzed at 32dpf had only testes that possessed spermatogonia (sg) and spermatocytes (sc) but lacked later developmental stages (spermatids and sperm) (Figure 4I). In addition, 32dpf mutant gonads showed abnormal clusters of cells with pyknotic nuclei (pc, outlined by dashed lines in Figure 4I) and contained tubules abnormally depleted of germ cells (asterisk, Figure 4I).

The lack of perinucleolar oocytes in *brca2* mutant gonads during the critical period for sex determination is consistent with the finding that gonads lacking oocytes during this period assume a male fate [20]. In addition, results showed that *brca2* mutant germ cells became pyknotic, disappeared, and left empty spermatogenic tubules.

brca2 Spermatocytes Undergo Apoptosis

The presence of pyknotic spermatocytes, lack of spermatids and sperm, and the existence of empty tubules in *brca2* mutant testes suggested the hypothesis that spermatocytes did not progress through meiosis and died. To test if the activation of apoptotic pathways is involved in spermatocyte death, we used immunoassays to detect active-Caspase-3, a marker of apoptosis [50]. In contrast to wild-type gonads, *brca2* mutant testes showed clusters of cells with active-Caspase-3 that were clearly pyknotic after hematoxylin and eosin staining (Figure 4J–4M), confirming that *brca2* spermatocytes undergo apoptosis.

Immature *brca2* Gonads Have a Male-Expression Profile

At 47dpf, *brca2*(*fancd1*) mutants already showed hypogonadism (Figure S6I), a characteristic shared by many FA patients. Germ cell distribution as revealed by *vasa* expression [51] was similar in mutants and wild-type gonads (Figure S6A, S6E, S6I). In mutants, somatic cells expressing the Sertoli cell marker *amh* (*anti-Müllerian hormone*) [52,53] failed to form neat borders surrounding tubules as

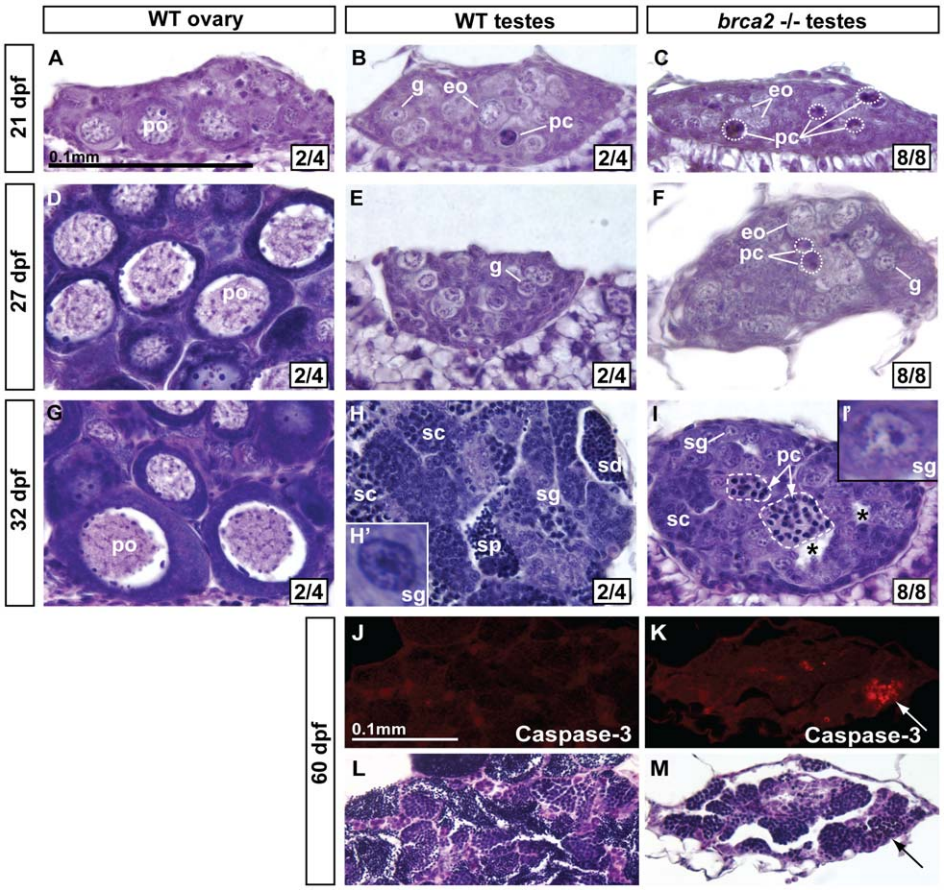

Figure 4. Developing gonads of *brca2* mutants lack perinucleolar oocytes and develop testes that contain pyknotic and apoptotic cells. In transitioning gonads of wild types at 21dpf, ovary-like gonads (A) contained perinucleolar oocytes (early stage IB), while testis-like gonads (B) contained gonia, some early oocytes, and a few pyknotic cells. (C) Gonads of 21dpf *brca2* mutants contained a few early oocytes and many pyknotic cells. (D) By 27dpf, perinucleolar oocytes had enlarged in wild-type ovaries. (E) Wild-type 27dpf testes possessed gonia. (F) 27dpf *brca2* mutant gonads contained gonia, some early oocytes (judging from cell size and the location and number of nucleoli), showed testis-like morphology, and had many pyknotic cells. (G) At 32dpf, wild-type immature ovaries contained growing perinucleolar oocytes that had reached diplotene stage (late stage IB). (H) Wild-type 32dpf testes showed germ cells at all stages of spermatogenesis: spermatogonia, spermatocytes, spermatids, and sperm. (I) Homozygous *brca2* mutant gonads at 32dpf possessed spermatogonia and spermatocytes, and tubules filled with pyknotic cells (dashed area) but lacked spermatids and sperm and had instead empty tubules (*). In transitioning gonads at 21–27dpf, we use the term 'gonia' (g) to represent cells that show the histological characteristics of spermatogonia (central nucleolus) and in differentiating testes at 32 dpf, we used the term 'spermatogonia' (sg) to represent such cells (Figure 4H', 4I'). (J) Anti-active-Caspase-3 staining did not label cells in immature 60dpf wild-type testes. (K) In contrast, anti-active-Caspase-3 stained cohorts of cells in immature 60dpf mutant testes. (L,M) Staining the same sections with hematoxylin and eosin showed that cells staining for anti-active-Caspase-3 were pyknotic (arrows). Oocyte staging according to [49]. Magnification bar for A-I shown in A and for J-M shown in J. Abbreviations: asterisks (*), empty testis tubules; eo, early oocyte; pc, pyknotic cells; po, perinucleolar oocyte; sc, spermatocytes; sd, spermatids; sg, spermatogonia; sp, sperm.
doi:10.1371/journal.pgen.1001357.g004

in wild-type males (Figure S6F,S6J) and lacked expression of the female marker *cyp19a1a* (*aromatase*) [54] (Figure S6C, S6G, S6K). The early meiotic marker *sycp3* (*synaptonemal complex protein 3*, [55]) was expressed by groups of spermatocytes in wild-type and mutant males (Figure S6H, S6L). We conclude that mutant gonads develop a molecular profile similar to wild-type testis accompanied by disorganization of *amh*-expressing somatic cells that surround testis tubules.

Neoplasia and Impaired Spermatogenesis in Adult Mutant Testes

To understand the cellular basis of male infertility in *brca2* mutants, we compared adult testis histology in wild types (n = 3) and *brca2* mutants (n = 7). Comparison of the anterior part of the testes (anterior testes) of wild types and *brca2* mutants revealed persistent hypogonadism (smaller diameter gonads) in the mutants (Figure 5A, 5B). Strikingly, *brca2* mutant testes lacked sperm and showed tubules with central empty cavities (asterisks). Wild-type and mutant testes both contained spermatocytes at the bouquet stage (late-zygotene/early-pachytene [56,57]) (sc-b, Figure 5C, 5D), but mutants lacked later stages (spermatids and sperm). Mutant testes also contained abnormal clusters of pyknotic cells (pc, Figure 5D). Occasionally, bouquet stage spermatocytes and pyknotic cells occupied the same tubule (Figure 5E), suggesting that spermatocytes blocked in meiosis became pyknotic. Eosinophils (eos, Figure 5F) invaded some cavities containing pyknotic cells, suggesting an inflammation-like response in mutant gonads. In the posterior part of the testes (posterior testes) of wild types, tubules demarcated by interstitial cells were filled with sperm (sp, Figure 5G), but in the posterior testes of *brca2* mutants, tubules were devoid of sperm (Figure 5H). This observation can account for the infertility phenotype of adult *brca2* mutant males.

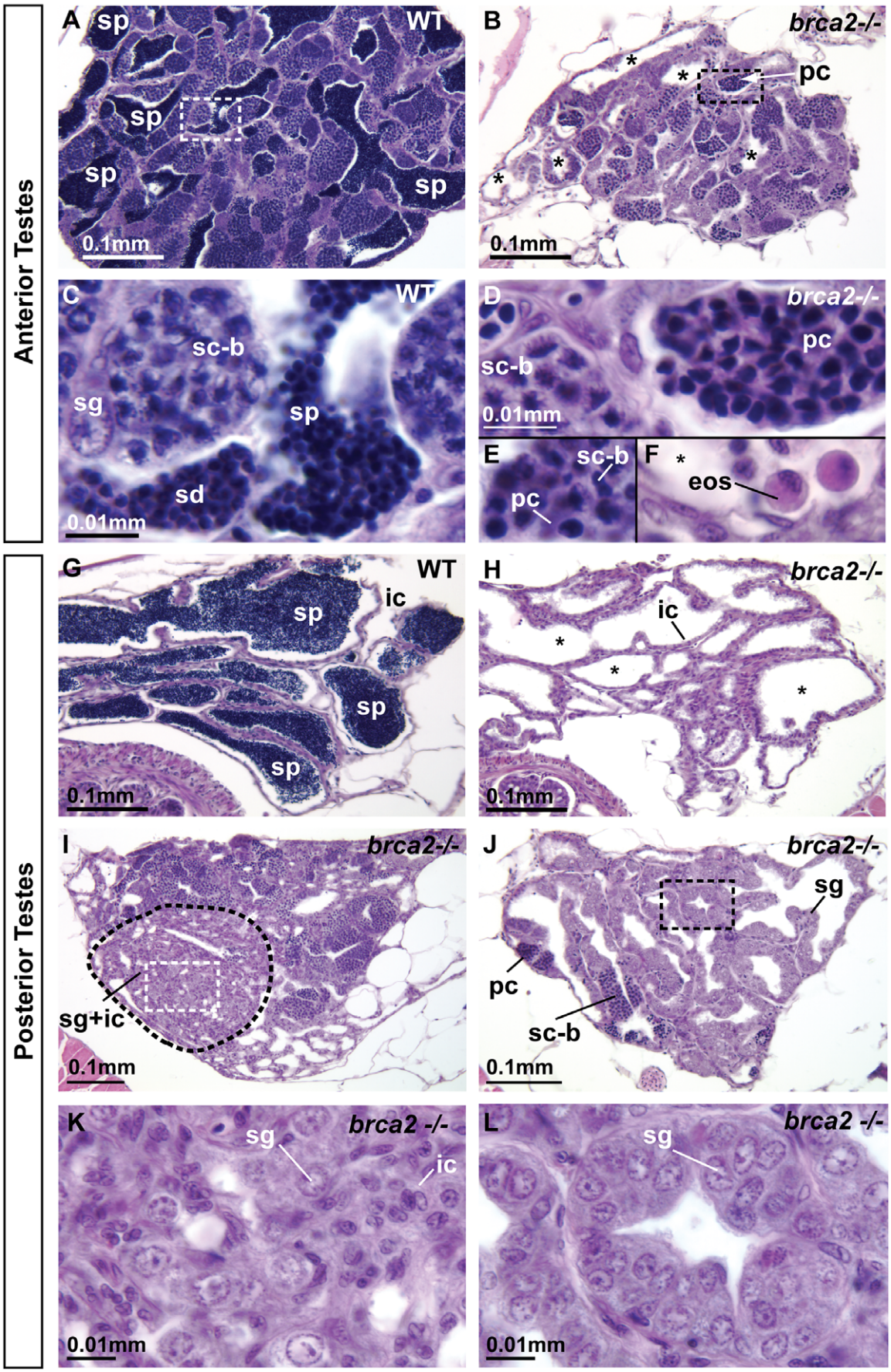
Anterior Testes
Posterior Testes
A
sp
WT
sp
sp
sp
0.1mm
B
brca2-/-
pc
0.1mm
C
WT
sc-b
sg
sp
sd
0.01mm
D
brca2-/-
pc
sc-b
0.01mm
E
sc-b
pc
F
eos
G
WT
ic
sp
sp
sp
0.1mm
H
brca2-/-
ic
0.1mm
I
brca2-/-
sg+ic
0.1mm
J
brca2-/-
sg
pc
sc-b
0.1mm
K
sg
brca2 -/-
ic
0.01mm
L
sg
brca2 -/-
0.01mm

Figure 5. Adult *brca2* mutant testes showed meiotic arrest and lack of spermatids and sperm and developed neoplasias. (A) Adult testes of wild types were organized into tubules that contained sperm (sp). (B) Adult testes of *brca2* mutants were smaller in diameter and lacked sperm, but instead contained clusters of pyknotic cells and empty tubules (asterisks). (C) The anterior part of the testes (anterior testes) in wild-type adults possessed all stages of spermatogenesis: spermatogonia, spermatocytes at the bouquet stage (late zygotene-early pachytene) of meiosis, as well as later stages -- spermatids and sperm. (D,E,F) *brca2* mutant anterior testes also had spermatogonia and bouquet stage spermatocytes, but strikingly, contained tubules of pyknotic cells, lacked spermatids and sperm, and had eosinophils that were not observed in wild-type testes. (G) The posterior part of the testes (posterior testes) of wild types contained tubules filled with germ cells at only the latest stage of spermatogenesis: sperm. (H) The posterior testis of *brca2* mutants lacked sperm and had empty tubules (*) formed by interstitial cells. (I,J) The posterior testes of *brca2* mutants developed neoplasias formed by spermatogonia and interstitial cells, demarcated by dotted lines and shown in enlargements (K,L). Abbreviations: asterisks (*), empty testis tubules; eos: eosinophils; ic: interstitial cells; pc: pyknotic cells; sc-b: spermatocytes at bouquet stage; sd: spermatids; sg: spermatogonia; sp: sperm.
doi:10.1371/journal.pgen.1001357.g005

In addition to truncated spermatogenesis, *brca2* mutant testes displayed abnormal regions of accumulating cells (Figure 5I-5L). Some of these neoplasias contained both spermatogonia (sg) and interstitial cells (ic, Figure 5I, 5K) and others contained only spermatogonia (sg, Figure 5J, 5L). We conclude that *brca2* provides some function that regulates proliferation of spermatogonia and interstitial cells.

Sertoli Cells Are Altered in Adult Mutant Testes

To help understand the altered morphologies of adult mutant testes, we studied gene expression patterns. In the anterior testis, *brca2* mutants contained more clusters of *vasa*-expressing cells than did wild types (Figure 6A, 6A′, 6D, 6D′), reflecting the accumulation of *vasa*-expressing early germ cell stages (spermatogonia and spermatocytes, Figure 6A′, 6D′)) and the depletion of non-*vasa* expressing late stages (spermatids and sperm; purple circle, Figure 6A′). In *brca2* mutants, *amh*-expressing cells were less frequent and did not surround tubules normally (Figure 6B, 6E). In addition, *sycp3*-expressing pachytene spermatocytes accumulated abnormally in mutant testes (Figure 6C, 6F), as expected from the histological data that showed the lack of post-meiotic cells.

The posterior testes of adult wild types did not express *vasa* and *amh*, consistent with the presence of interstitial cells and late germ cells (sperm), which no longer express *vasa*, and the absence of Sertoli cells (Figure 6G–6I). In contrast, posterior testes of adult mutants contained empty cavities and abnormally proliferating cells (Figure 6J–6O) similar to those observed in histological analyses (Figure 5I–5L). Neoplasias contained either mixtures of *vasa*-expressing and non-*vasa*-expressing cells (Figure 6J–6L) or possessed only *vasa*-expressing, early spermatogenic cells (Figure 6M–6O). These results revealed the abnormal presence of early spermatogenic cells in the posterior part of the testes in mutants. Moreover, the presence of scattered *amh*-expressing cells revealed the abnormal presence of Sertoli cells in mutant posterior testes (Figure 6K, 6N).

Mutation of *tp53(p53)* Rescues *brca2* Sex Reversal

All zebrafish gonads initially form oocytes but these die in wild-type juvenile males [47,48], and increased germ cell apoptosis leads to oocyte loss and female-to-male sex reversal in *fancl* mutant zebrafish [20]. Tp53 (alias p53) is an important activator of apoptosis and zebrafish with hypomorphic mutations in *tp53* are viable and fertile despite reduced apoptosis [58,59]. To learn the role of apoptosis in sex reversal of *brca2* mutants, we made double mutants for *brca2* and the hypomorphic allele $tp53^{M214K}$ [58,59]. Results showed that no $brca2^{-/-}$ mutants with at least one wild-type *tp53* allele developed into females (Figure 7A). In contrast, $brca2^{-/-}$ mutants that lacked a normal *tp53* allele became males and females with about equal frequency (Figure 7A). This result shows that a *tp53* mutation can rescue the female-to-male sex reversal caused by the lack of *brca2* activity. Because double mutant females develop ovaries containing oocytes (Figure 7E), we conclude that Tp53-mediated apoptotic cell death is important for sex reversal in *brca2* mutants and interpret these results to mean that the survival of oocytes in *brca2* mutant gonads can allow individuals to become females. The rescue of sex reversal by Tp53 mutation reveals that *brca2* function is required for oocyte survival, which secondarily leads to female gonad fate and ovarian development.

Brca2 Function Is Not Required to Localize Animal or Vegetal Transcripts in Developing Oocytes

In wild-type late stage II to early stage III oocytes, *brca2* and *pou5f1* transcripts localize to the animal pole and *vasa* transcripts gradually spread out cortically from the vegetal pole (Figure 2G, 2H, Figure S7A–S7C, and [41,42,60-62]). To test the hypothesis that *brca2* function is important for the localization of these transcripts, we examined mRNA distribution in oocytes of *brca2;tp53* double mutants. In situ hybridization on adjacent serial sections showed that double mutant females produced oocytes with *brca2* and *pou5f1* transcripts localized to one pole and *vasa* transcripts positioned at the opposite pole of the same individual oocytes (Figure S7D–S7F). We conclude that *brca2* activity is not necessary to localize the messages tested to their proper location in developing zebrafish oocytes.

Mutation of *tp53* Does Not Rescue Infertility in *brca2* Mutants

To learn if *tp53* mutation can rescue the infertility phenotype observed in *brca2* single mutants, we mated *brca2* homozygous mutants that were either wild type, heterozygous, or homozygous for the *tp53* mutation to wild-type animals and scored fertility. Results showed that all *brca2* mutant males were sterile regardless of their *tp53* genotype (for $brca2^{-/-}$;$tp53^{+/+}$, $brca2^{-/-}$;$tp53^{+/-}$, and $brca2^{-/-}$;$tp53^{-/-}$: we found 0/200 offspring (8 males tested), 0/349 offspring (13 males tested), and 0/148 offspring (6 males tested), respectively). Female *brca2*;*tp53* double mutants were also sterile when mated to wild-type males (of 549 eggs produced by 9 females, 79 initiated cleavage (the average double mutant female had 20%±18% fertility compared to doubly heterozygous siblings with 85%±27% fertility). Non-developing eggs laid by double mutant females were milky and were of highly variable size. Some double mutant females mated to wild-type males produced doubly heterozygous eggs that completed cleavage and gastrulation, but failed to develop to later stages (Figure 7B). Because doubly heterozygous individuals from doubly heterozygous mothers develop normally but doubly heterozygous embryos from homozygous *brca2* mutants are lethal, and because homozygous *tp53* mutant females have normal fertility [58], we conclude that maternal *brca2* function is important for proper embryo development.

Oocytes in *brca2;tp53* Double Mutants Have Altered Nuclear Architecture

Histological sections of 6mpf (months post-fertilization) adult ovaries from wild types ($brca2^{+/+}$;$tp53^{+/+}$; n = 3), *tp53* homozygous

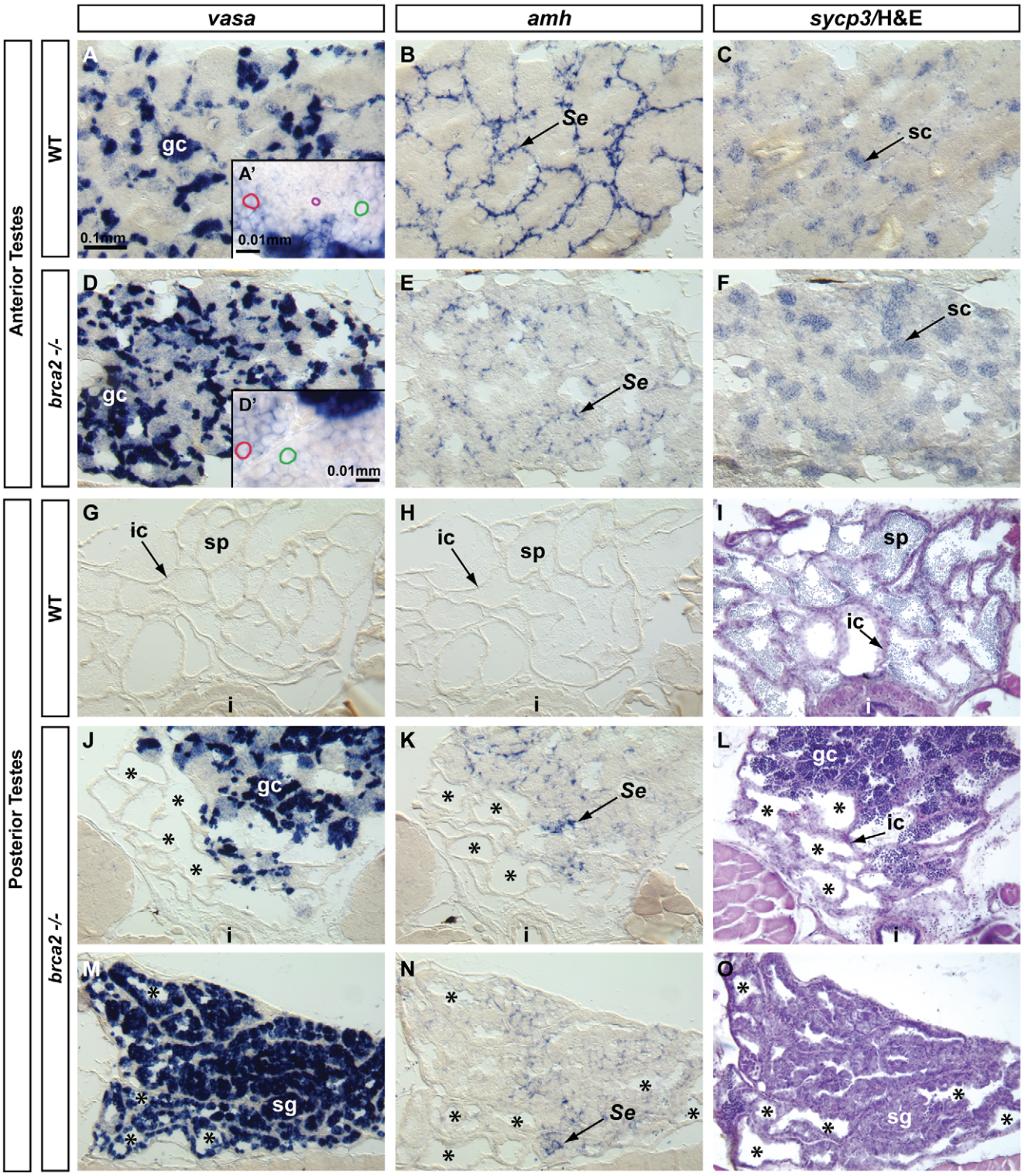

Figure 6. Altered Sertoli cell distribution, proliferation of spermatogonia, and accumulation of recombination-phase spermatocytes in *brca2* mutant testes. *In situ* hybridization on adjacent sections of testes with markers for early germ cells (*vasa*), Sertoli cells (*amh*) and germ cells during recombination stages (*sycp3*) in wild types and *brca2* mutants. (A–C) The anterior testis of wild types expressed *vasa* in early germ cells, *amh* in Sertoli cells surrounding tubules, and *sycp3* in meiotic spermatocytes. (A′) Enlargement illustrates a gradient of *vasa* expression in spermatocytes: from moderate *vasa* expression (red circle) to low *vasa* expression (green circle), and finally spermatids and sperm (purple circle) that did not express *vasa*. (D) The anterior testis of *brca2* mutants showed more tubules with *vasa*-expressing spermatogonia than wild types (A). (D′) Enlargement shows cells expressing low levels of *vasa* (red circle) and spermatocytes not expressing *vasa* (green circle) but no small spermatids or sperm. (E) *brca2* mutants showed that *amh*-expressing cells were poorly organized and did not surround tubules neatly as in wild types, revealing an altered Sertoli cell distribution. (F) *brca2* mutants expressed the recombination marker *sycp3* in locally larger cell clusters than wild types, revealing an increased local concentration of cells at or entering pachytene stage. (G, H) In the posterior part of the testis, wild types did not

express *vasa* or *amh*. (I) Hematoxylin and eosin (H&E) staining clearly showed sperm in many tubules in the posterior testes of wild types. (J–O) The posterior testes of *brca2* mutants contained many tubules that were devoid of sperm (*) and contained *vasa*-expressing germ cells and Sertoli cells, which are not normally found in the wild-type posterior testes. (M–O) In one of two mutants analyzed, the posterior testes contained a larger proliferation of *vasa*-positive spermatogonia and also showed disorganized *amh*-expressing Sertoli cells, lacked sperm, and had empty tubules. Abbreviations: asterisks (*), empty testis tubules; gc, germ cells; i, intestine; ic, interstitial cells; sg, spermatogonia; sc, spermatocytes; *Se*, Sertoli cells; sp, sperm.
doi:10.1371/journal.pgen.1001357.g006

mutants (*brca2*$^{+/+}$;*tp53*$^{-/-}$; n = 3) and double mutants (*brca2*$^{-/-}$;*tp53*$^{-/-}$; n = 4) revealed oocytes at a variety of developmental stages in all three genotypes (Figure 7C–7E). In *tp53* mutants and in wild types, late stage IB oocytes (L-IB) contained nucleoli distributed uniformly along the nuclear periphery (Figure 7C, 7D, 7D′), consistent with the normal fertility of homozygous *tp53*^{M214K} mutants [58]. In contrast, *brca2;tp53* double mutants contained degenerating late stage oocytes (d, Figure 7E) with a granulosa cell layer (gc) that was poorly organized and sometimes separated from the vitelline envelope (ve, Figure 7E′). Wild-type nuclei of late stage IB to early stage II, stage II, and stage III oocytes were radially symmetrical, containing peripheral nucleoli and central chromosomes (Figure 7F–7H). In contrast, *brca2*$^{-/-}$;*tp53*$^{-/-}$ double mutant oocytes were polarized, showing abnormally enlarged and variably shaped nucleoli that accumulated asymmetrically towards one pole of the nucleus while chromosomes concentrated towards the opposite pole (Figure 7I–7K). We conclude that *brca2* activity is essential to establish or to maintain a normal architecture of the oocyte nucleus.

In addition to their abnormal location, oocyte chromosomes in double mutants had altered morphology. In wild-type oocytes, chromosomes were distributed independently in the center of the nucleus (arrows in Figure 7L), but chromosomes in oocytes of double mutants were interconnected and formed abnormal loops (arrows in Figure 7M). These chromosome phenotypes were not observed in oocytes of *tp53* single mutant females. Aberrant chromosome structure would be expected if recombination-induced chromosome breaks are left unrepaired or are repaired by an error-prone pathway. Our experiments showed that MMC-induced DNA breaks caused chromatid and chromosome damage that led to radial reunion formation in somatic cells (Figure 3I). Likewise, inappropriate repair of recombination-induced DNA breaks could prevent dispersal of oocyte chromosomes. These results suggest a role of *brca2* in repairing DNA breaks originating either artificially by MMC or naturally in meiotic recombination.

Ovarian Tumors in *brca2;tp53* Double Mutants

Because humans heterozygous for *BRCA2* mutations have elevated risk of tumors, we investigated older *brca2:tp53* mutants for abnormal growths. By 6mpf, tumors formed that invaded the ovarian cavity and intercalated between oocytes in two of four *brca2*$^{-/-}$;*tp53*$^{-/-}$ double mutants examined (asterisks, Figure 7N–7Q). Tumors were not detected in wild types (n = 3) or in *tp53* homozygous mutants (n = 3). One tumor appeared to originate at the ovarian cavity membrane (arrow, Figure 7N). Tumor origin in the other female was unclear because it was metastatic and contacted both the ovarian cavity membrane and the swim bladder (Figure 7P). Both tumors involved spindle-shaped cells that invaded the ovary and surrounded the oocytes (Figure 7N′, 7O, 7Q). The high incidence of ovarian cancer we observed in *brca2*$^{-/-}$;*tp53*$^{-/-}$ double mutants contrasts with the prior finding that animals homozygous for either of two mutant *tp53* alleles (*tp53*^{M214K}, the mutation used here, or *tp53*^{I166T}) are viable and fertile, but at 8.5 or 8.8mpf (ten weeks later than our double mutants), 1 of 144 and 1 of 417 fish, respectively, began to show tumors and by 16.5 or 22mpf, 28% or 100%, respectively, of the *tp53* mutants had developed tumors [58,59]. Of several hundred tumors previously described in *tp53* mutants, none were reported to involve the ovarian cavity membrane [58,59]. The early appearance and unique ovarian location of tumors in *brca2*$^{-/-}$;*tp53*$^{-/-}$ double mutants suggest a specific association with *brca2* activity, potentiated by impaired *tp53* function and Tp53 deficiency is cooperative with Brca2 in tumorigenesis in humans [8]. Future long-term investigations are required that focus on tumor development in a large cohort of *brca2*$^{-/-}$;*tp53*$^{-/-}$ double mutants (1/16th of the progeny of double heterozygotes) compared to their single mutant *tp53*$^{-/-}$ siblings to more clearly define the role of *brca2* in the development of ovarian tumors.

Neoplasia and Megalospermatogonia in *brca2;tp53* Double Mutants

Testis development was abnormal in double mutants. Analyses of wild-type (n = 4) and *tp53* single mutant (n = 3) testes in 6mpf adults revealed germ cells at all stages of spermatogenesis in all the animals analyzed (Figure 8A, 8B). In contrast, all testes analyzed of *brca2*−/− single mutants (*brca2*$^{-/-}$;*tp53*$^{+/+}$; n = 4) and double mutants (*brca2*$^{-/-}$;*tp53*$^{-/-}$, n = 6) abnormally lacked spermatids and sperm (Figure 8C, 8D). Furthermore, in all *brca2*$^{-/-}$;*tp53*$^{+/+}$ single mutants and all *brca2*$^{-/-}$;*tp53*$^{-/-}$ double mutants, posterior tubules contained empty cavities lacking germ cells (asterisks in Figure 8C, 8D) consistent with our finding that adult double mutants failed to recover fertility. Unexpectedly, some testes in *brca2*$^{-/-}$;*tp53*$^{-/-}$ double mutants (n = 2), but not in the other genotypes, contained germ cells enlarged up to ten times normal diameter (Figure 8E). Some of these enormous cells we call megalospermatogonia (ms) because, like normal spermatogonia [63], they contained an enlarged central nucleolus (nc). Testes of some *brca2*$^{-/-}$;*tp53*$^{-/-}$ double mutants (n = 3) contained other large cells that showed the peripheral distribution of numerous nucleoli, which constitutes an oocyte-like morphology [63], so we interpret these as large early oocytes (eo), and additionally we observed the presence of enlarged pyknotic cells (pc) (ms, pc, and eo in Figure 8E, 8F, 8F′, compare to normal spermatogonia (sg) outlined by dashed lines in Figure 8E, 8F). The lack of sex-specific markers for early gonial cells precludes a more precise definition of cell type. Somatic cell neoplasias appeared in the posterior testis of all double mutants (but showing variability on the neoplastic tissue size) (Figure 8G, 8G′) suggesting the hypothesis that late stage spermatogenic cells negatively regulate the proliferation of somatic cells in testes. To test this hypothesis and to investigate whether the absence of *brca2* activity or merely the absence of germ cells allows over-proliferation of the somatic component of the testis, we examined animals depleted of germ cells by *dead end*-morpholino (*dnd*−/−; n = 10; see also [64]). Dnd is an RNA binding protein that is essential for germ cell survival in mice and zebrafish [64,65]. Our results revealed that testes in 18mpf *dnd*-morpholino treated animals developed neoplastic somatic proliferation (Figure 8H, 8H′) similar to those observed in *brca2* single and *brca2;tp53* double mutants (Figure 5I, 5K, Figure 8G). In five of ten *dnd*-injected animals, neoplasias invaded the intestine and body wall musculature (Figure 8H). Although we did not detect invasive somatic proliferation in *brca2* mutants, these *dnd*-knockdown animals were 12 months older than our *brca2* mutants, suggesting that invasive proliferation might arise in *brca2* mutants as they age.

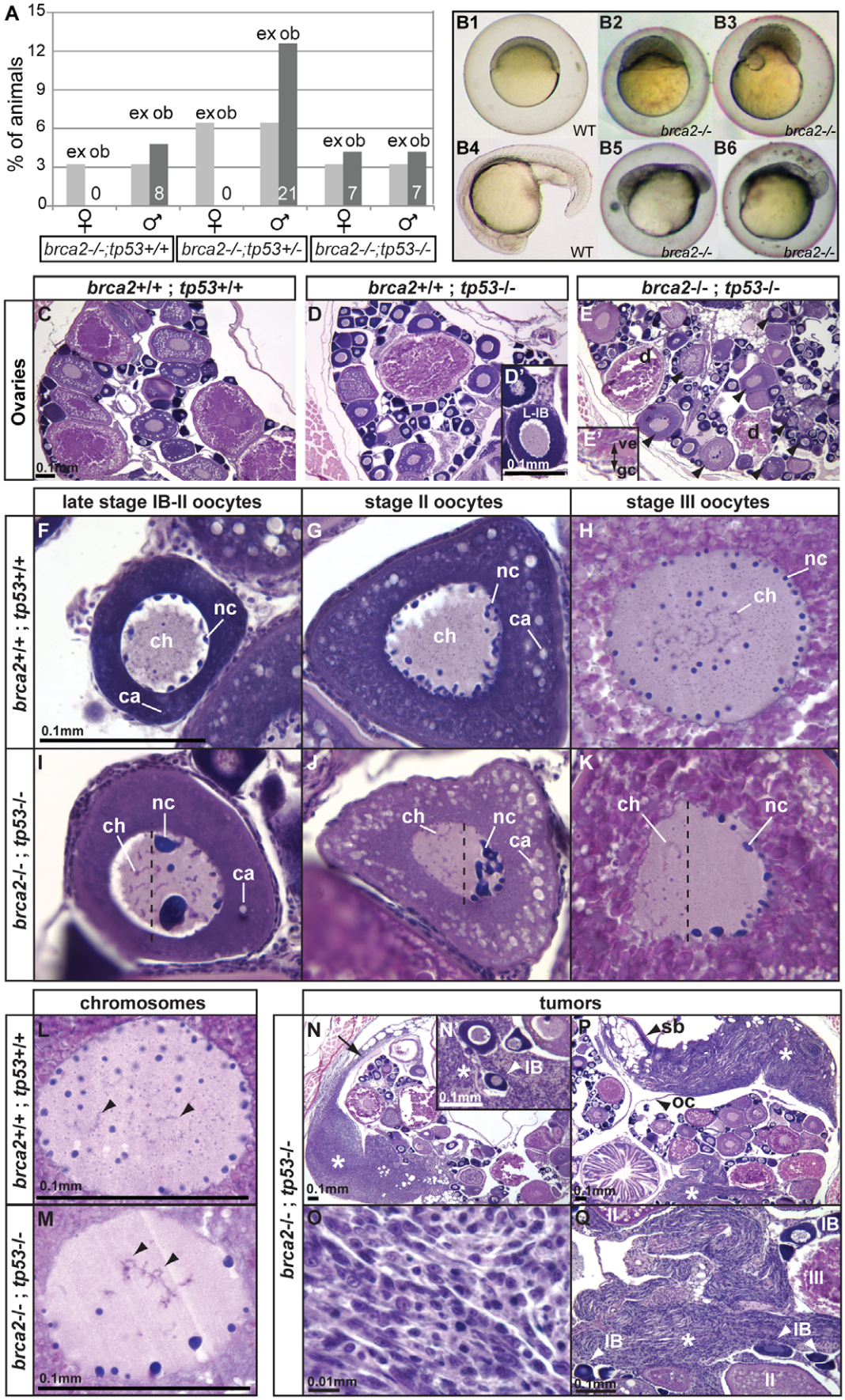
A
% of animals
15
12
9
6
3
0
ex ob
0
ex ob
8
ex ob
0
ex ob
21
ex ob
7
ex ob
7
♀
♂
♀
♂
♀
♂
brca2-/-;tp53+/+
brca2-/-;tp53+/-
brca2-/-;tp53-/-
B1
B2
B3
WT
brca2-/-
brca2-/-
B4
B5
B6
WT
brca2-/-
brca2-/-
brca2+/+ ; tp53+/+
brca2+/+ ; tp53-/-
brca2-/- ; tp53-/-
Ovaries
C
0.1mm
D
D'
L-IB
0.1mm
E
d
d
E'
ve
gc
late stage IB-II oocytes
stage II oocytes
stage III oocytes
brca2+/+ ; tp53+/+
F
nc
ch
ca
0.1mm
G
nc
ch
ca
H
nc
ch
brca2-/- ; tp53-/-
I
nc
ch
ca
J
ch
nc
ca
K
ch
nc
chromosomes
tumors
brca2+/+ ; tp53+/+
L
0.1mm
brca2-/- ; tp53-/-
M
0.1mm
N
N'
IB
0.1mm
0.1mm
P
sb
oc
0.1mm
O
0.01mm
Q
II
IB
III
IB
IB
II
0.1mm

Figure 7. Mutation of *tp53* rescued the *brca2* sex reversal phenotype, yielding infertile double-mutant females that produced ovaries containing oocytes with altered nuclear architecture that developed into defective embryos and that produced invasive ovarian tumors. (A) Expected (ex) and observed (ob) frequencies of various *tp53* genotypes among the homozygous *brca2* mutant offspring of parents doubly heterozygous for $tp53^{M214K}$ and $brca2^{ZM\_00075660}$ alleles. Females developed only in the absence of a wild-type *tp53* allele, showing that the *tp53* mutation rescued the sex reversal phenotype. (B) Doubly heterozygous embryos from the mating of homozygous *tp53* females to males heterozygous for the *brca2* mutation develop like normal embryos (B1 and B4 at 6 and 19 hpf, respectively) but the same genotype developing from the mating of rescued *brca2;tp53* double mutant females and homozygous wild-type males stopped developing shortly after gastrulation (B2, B3, B5, B6). (C–E) Sections of ovaries from 6mpf wild-type, single mutant *tp53*, and double mutant *brca2;tp53* adults, respectively, showed that oocytes in *tp53* mutants developed normally (D′) but that oocytes degenerated and the vitelline envelope was abnormally separated from the granulosa cells in double mutants (E′). Strikingly, oocytes in double mutants showed nuclear anomalies (arrowheads in E). (F–H) Sections of wild-type late stage IB (transitioning to stage II), stage II, and stage III oocytes, respectively, contained radially symmetrical nuclei with small round nucleoli located mostly near the nuclear envelope and thin chromosomes separated from each other in the middle of the nucleus. (I–K) Sections of late stage IB, stage II, and stage III oocytes of *brca2;tp53* double mutants showed abnormal nuclear asymmetry. Oocytes contained nuclei with large, variably-shaped nucleoli clustered at one side of the periphery of the nucleus instead of the normal uniform distribution around the periphery of the nucleus and chromosomes clustered at the other side of the nucleus opposite to the nucleoli. (L) Chromosomes in wild types were thin and separated (arrowheads). (M) Chromosomes in oocytes of double mutants were thicker and clumped and formed abnormal crosses and loops (arrowheads). (N,P) Invasive ovarian tumors (asterisks) were detected in sections of two of four *brca2;tp53* double mutants by 6mpf but were not present in other genotypes (wild-types and single *tp53* mutants). (N) One tumor appeared to originate at the ovarian cavity membrane (arrow) and the other tumor (P) was metastatic and contacted the ovarian cavity membrane and the swim bladder. (N′,Q) Both tumors were formed by spindle-shaped cells (O) that invaded the ovary and surrounded the oocytes. Abbreviations: IB,II,III: oocyte stages; ca, cortical alveoli; ch, chromosomes; d, degenerating oocyte; gc, granulosa cell; nc, nucleoli; oc, ovarian cavity; sb, swim bladder; ve, vitelline envelope.
doi:10.1371/journal.pgen.1001357.g007

Overall, these results would be expected if somatic cell neoplasias in *brca2* and *brca2;tp53* mutants were not due to a direct effect of the lack of *brca2* activity, but arose as a secondary effect of germ cell loss in *brca2* mutants. A possible mechanism to explain these results is that late stage germ cells in the wild-type spermatogenic pathway exert a negative control over the proliferation of somatic cells in zebrafish testes. Loss of Dead end function in mouse results in germ cell tumors in a strain-specific manner [65]. Because *dnd*-knockdown zebrafish have no germ cells, the origin of gonad tumors after *dnd*-knockdown differs between mouse and zebrafish. Long-term investigations are required to examine whether the somatic testicular tumors we observed in zebrafish lacking *dnd* function are subject to effects of the genetic background.

Discussion

The biological mechanisms that underlie Fanconi anemia and hereditary breast, ovarian, and prostate cancer intersect at *Brca2*(*Fancd1*). Null alleles of *Brca2* are embryonic lethal in mouse and human [11,23,66], which precludes study of the gene's full function in homozygous null-allele adults in these species. Rats lacking Brca2 activity are viable [10], but mammals are not favorable for a whole-animal small molecule screen for therapeutic substances related to Brca2 disease. Here we exploit a viable zebrafish *brca2* null-allele. We show that zebrafish *brca2* is the ortholog of human *BRCA2*, it shares important coding features with the human gene, and it is expressed in rapidly dividing and meiotic cells. Importantly, we show that *brca2* maintains genome stability in response to DNA damaging agents and it is essential for the survival of post-recombinant spermatocytes. Loss of *brca2* function causes female-to-male sex reversal that is rescued by mutating *tp53*, indicating that *brca2* subverts female development by apoptosis and is required for normal oogenesis. Unexpectedly, we found that *brca2* transcript localizes asymmetrically to the animal pole of wild-type oocytes and that *brca2* activity is essential for establishing or maintaining the architecture of the oocyte nucleus. Moreover, results showed that *brca2* activity is necessary in zebrafish as it is in humans to prevent ovarian tumors in the absence of *tp53* function. Therefore, this work validates the zebrafish *brca2* mutant as a useful tool for small-molecule screens to help discover potential therapeutic compounds for human patients.

A Zebrafish *brca2*-Null Allele Disrupts Genome Stability

Genomic and genetic evidence shows that zebrafish has a single-copy of *brca2* that is orthologous to its mammalian counterpart. We found that the zebrafish genome has duplicate copies of the human chromosome segment that contains *BRCA2*, and that these duplicates arose from the teleost genome duplication (TGD). In one of these duplicated segments, the *BRCA2* ortholog disappeared, leaving zebrafish with a single copy of *brca2*. About 75% of genes from the TGD event reverted to singletons [27], but all of the 13 zebrafish orthologs of FA pathway genes are present in single copy [25], which would happen rarely (2.4%) solely by chance. We conclude that evolutionary forces probably acted to reduce *brca2* and other FA pathway genes to single copy after the TGD. This finding is predicted by the duplication-degeneration-complementation hypothesis [67], which suggests that genes with simple tissue- and time-specific regulatory elements would be more likely to revert to singletons than those with complex regulation. In addition, many Fanc proteins join to form molecular machines in a 1:1 stoichiometry, so that if one gene in the network evolves to single copy, the others might follow by natural selection or neutral evolutionary forces.

Expression analyses showed that maternal *brca2* message accumulated in zebrafish embryos. This message would be available to provide embryos with Brca2 protein that could function to help resolve stalled replication forks [68] during the rapid cleavage divisions that precede the mid-blastula transition, the stage at which zygotic transcription initiates [69]. Our finding that the heterozygous offspring of homozygous *brca2* mutant mothers fail to develop much past gastrulation supports this conclusion. Expression of *brca2* in meiotic cells of zebrafish, as in mammals [24], suggests a role in the repair of DNA breaks incurred during meiotic homologous recombination [46].

Zebrafish $brca2^{ZM\_00075660}$ mutants generate only aberrant transcripts that lack domains essential for Brca2 activity and provide a vertebrate null allele model to unravel the effects of *brca2* during embryonic and post-embryonic development. Mutant tissue culture cells and developing embryos show more chromosome damage and excess staining of broken DNA, respectively, than wild-type cells or embryos after exposure to DNA damaging agents. Similarly, loss of *BRCA2* function in humans results in hypersensitivity to DNA crosslinking agents [44,70], thus leading to chromosome breaks [43,71], showing that zebrafish and human *Brca2* orthologs share functions in maintaining genome stability.

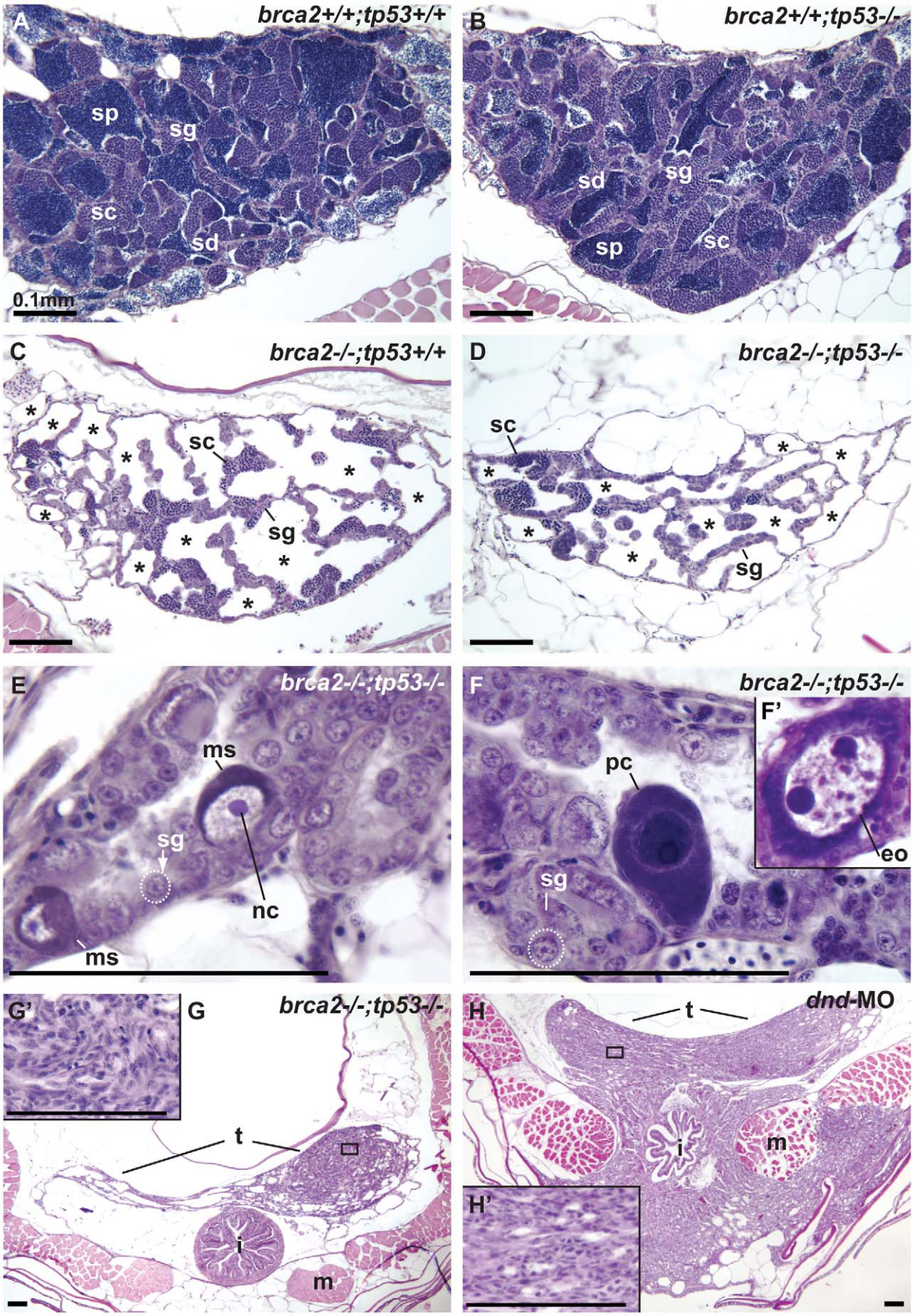
A
brca2+/+;tp53+/+
sp
sg
sc
sd
0.1mm
B
brca2+/+;tp53-/-
sd
sg
sp
sc
C
brca2-/-;tp53+/+
sc
sg
D
brca2-/-;tp53-/-
sc
sg
E
brca2-/-;tp53-/-
ms
sg
nc
ms
F
brca2-/-;tp53-/-
F'
pc
eo
sg
G'
G
brca2-/-;tp53-/-
t
i
m
H
dnd-MO
t
i
m
H'

Figure 8. Mutation of *tp53* failed to rescue infertility in *brca2* mutants. (A,B) Wild-type testis and *tp53* single mutant testis showed germ cells at all stages of spermatogenesis: spermatogonia, spermatocytes, spermatids and sperm. (C) *brca2* single mutant testis contained spermatogonia and spermatocytes, lacked spermatids and sperm and had large regions devoid of germ cells (asterisks). (D) Testes in *brca2;tp53* double mutants were similar to the *brca2* single mutant, but had additional developmental problems. (E) Double mutant testis formed large cells with a single central nucleolus like spermatogonia (called here megalospermatogonia). (F) Some of these abnormally enlarged cells were pyknotic and some showed an oocyte-like morphology similar to early oocytes (inset). (G) Double mutants showed neoplastic regions of abnormal somatic cell proliferation in the posterior regions of the testes that were depleted of sperm. (G′) Enlargement of the somatic proliferation of double mutant testes. (H) Genetically wild-type testes depleted of germ cells due to *dnd* morpholino knockdown formed neoplasms of somatic cells of the testis similar to the ones observed in *brca2;tp53* double mutants, but that invaded the intestine and muscle at older stages. (H′) Enlargement of the somatic proliferation of *dnd* testes. Abbreviations: asterisks (*), empty testis tubules; eo: early oocyte; i, intestine; m, muscle; ms, megalospermatogonia; nc, nucleolus; pc, pyknotic cell; sc, spermatocytes; sd, spermatids; sg, spermatogonia; sp, sperm; t, testis.
doi:10.1371/journal.pgen.1001357.g008

Flow cytometry showed that the poor growth of zebrafish *brca2* mutant cell cultures results from high rates of spontaneous apoptotic cell death. This finding parallels our finding of increased apoptosis in juvenile mutant gonads that results in oocyte loss and sex reversal and that the inhibition of cell death in *brca2;tp53* double mutants rescues sex reversal. Spontaneous apoptosis leading to bone marrow failure is also a problem in hematopoietic stem cells in human FA patients, [21]. Zebrafish therefore appears to be a valid model to study the basic influence of Brca2 deficiency on apoptosis. In contrast, the effect of damage caused by MMC in zebrafish *brca2* mutant cell cultures on non-apoptotic cell death rates is surprisingly low compared to humans; the cause of which remains unexplained.

Lack of Brca2 Activity Results in Female-to-Male Sex Reversal

Results showed that *brca2* mutant zebrafish developed exclusively as males due to female-to-male sex reversal. Sex ratios also appear to be skewed in the offspring of human carriers of *BRCA2* mutations, suggesting a possible role in sex determination or differential survival [72]. During the sex determination period, zebrafish mutant gonads contained apoptotic cells and lacked diplotene oocytes, the presence of which is essential to tip gonad fate towards the female pathway in *fancl* zebrafish mutants [20]. In contrast to *fancl* mutants, which become fertile males, *fancd1*(*brca2*) mutants become sterile males. The more severe phenotype of *brca2* mutants compared to *fancl* mutants parallels the fact that human homozygotes for *FANCD1*(*BRCA2*) null alleles are lethal as embryos [11]. In the FA-BRCA network, FANCL should act upstream of BRCA2 (see for review [73]. Because the phenotype of *brca2* mutant zebrafish is more severe than that of *fancl* mutant zebrafish, BRCA2 likely plays roles in addition to its function downstream of *fancl*. Because *FANCD1*(*BRCA2*) is the only FA complementation group that fails to form RAD51 foci after ionizing radiation and crosslink damage, FANCD1(BRCA2), but not FANCL, is required for RAD51-mediated DNA repair [74,75].

The inhibition of apoptosis in *brca2* mutants by the mutation of *tp53* rescued female-to-male sex reversal and led to the development of females, consistent with the idea that *brca2* mutant oocytes die by apoptosis when unable to repair DNA breaks associated with meiotic recombination. This conclusion parallels that from zebrafish *fancl* mutants, in which oocytes die in juveniles followed by female-to-male sex reversal [20] and supports the notion that *fanc*-related sex reversal acts via Tp53-mediated apoptosis.

The *brca2*(*fancd1*) and *fancl* results combine to support the following model for zebrafish sex determination. (1) The FA network facilitates DNA repair associated with meiosis and hence the survival of oocytes during the critical period for zebrafish sex determination. (2) Activation of Tp53-dependent germ cell apoptosis, at least in *fanc* mutants, alters the total number of germ cells and thus reduces the number of surviving oocytes below the threshold necessary to maintain female fate. (3) Post-recombinant oocytes release a signal that down-regulates *amh* and/or maintains *cyp19a1a* (*aromatase*) expression in somatic cells of the bipotential gonad [20,48,52,64,76-80]; the fewer the number of post-recombinant oocytes, the less aromatase-maintenance signal. (4) Aromatase converts testosterone to estrogen, thereby reinforcing ovary development and the female fate. (5) In normally developing males at the juvenile hermaphrodite stage [47], unknown genetic factors that may be influenced by the environment stimulate the death of oocytes and hence loss of the aromatase-maintenance signal. According to this model, in the absence of either *brca2*(*fancd1*) or *fancl*, oocytes do not effectively repair the DNA breaks of meiosis, DNA-damaged oocytes die by apoptosis before they liberate the aromatase-maintenance signal, the gonad becomes a testis, and individuals that otherwise would have become females develop into males.

The study of zebrafish *brca2* mutants verifies the importance of *Brca2* for gonad development and provides a new vertebrate model for the adult roles of Brca2 that is obscured by null mutant lethality in human and mouse. Neither *Brca2* knockout rats nor *Brca2* knockout mice rescued by a human *BRCA2* BAC showed sex reversal [10,24], reflecting lineage-specific sex determining mechanisms. Zebrafish *brca2* mutants developed gonads without diplotene oocytes, but rescued mice did develop oocytes, many of which disappeared post-natally, but some of which progressed through meiotic prophase I, became fertilized, and produced embryos [24]; in contrast, *Brca2* mutant rats were sterile. A possible explanation for the difference between mouse and rat is that the transgenic mice might not be total null mutants because expression of human *BRCA2* was detected in their gonads [24].

Brca2 Activity Is Essential for Normal Spermatogenesis

Zebrafish *brca2* mutants contained spermatocytes arrested in meiosis, as did transgenic mice rescued by human *BRCA2* [24] and rats mutant for $Brca2^{-/-}$ [10]. We found that zebrafish *brca2* mutant testes (1) showed hypogonadism like human FA patients; (2) developed spermatogonia that entered meiosis as shown by *sycp3* expression and histological data; (3) contained bouquet stage spermatocytes that arrested in late zygotene-early pachytene; (4) lacked post-meiotic spermatogenic stages, including spermatids and sperm; (5) failed to properly organize Sertoli cells, as shown by *amh* expression; (6) contained abnormal pyknotic cells that were positive for the apoptotic marker active-Caspase-3; and (7) formed tubules that lacked germ cells but contained eosinophils, blood cells involved in inflammation. Together, these results suggest a mechanistic model in which *brca2* mutant spermatogenic cells develop rather normally until meiotic recombination (pachytene), fail to repair double strand DNA breaks associated with homologous recombination, then die, leaving empty testis tubules in hypogonadal sterile males.

Because spermatogenic cells die even in *brca2*;*tp53* double mutants, we conclude that, after meiotic failure, *brca2* spermatogenic cells die by a Tp53-independent pathway in double mutants, or alternatively, that the hypomorphic nature of the $tp53^{M214K}$ allele may allow cells to disappear by a Tp53-dependent pathway. Megalospermatogonia with enormous nuclei appeared in double mutants, possibly due to continued DNA replication in spermatogonia damaged by inadequate DNA repair in the absence of *brca2* activity. In *brca2* single mutant testes, cells may experience extra rounds of replication but *tp53*-mediated cell death may delete them. Alternatively, in the absence of *brca2* function, *tp53* activity might be required to prevent abnormal functions that lead to cell enlargement and megalospermatogonia. The presence of oocytes in testes of double mutant animals might be explained by the alteration of somatic cell-to-germ cell signaling in testes that are developing with abnormal Sertoli cell distribution and lack of spermatids and sperm. Normal Tp53 function might be necessary to induce oocyte apoptosis in *brca2* single mutant testes.

brca2 Mutant Testes, Neoplasia, and Germ Cell-to-Soma Signaling

Six-month old *brca2* single mutants accumulated neoplastic growths involving spermatogonia with or without disorganized clumps of interstitial cells. The posterior part of the testis, which completely lacked germ cells in *brca2* single and *brca2;tp53* double mutants, showed abnormal proliferation of somatic cells in the testes. The investigation of genetically wild-type animals lacking germ cells due to *dnd* knockdown uncovered somatic neoplasias of the testes similar to those found in *brca2* mutant testes. Knockdown of *dnd* was not previously reported to cause neoplasias, but the oldest *dnd*-knockdown animals previously reported were 6 months old [64] and our dnd-knockdowns were 18 months old, suggesting that these neoplasias arise with age, although we can't rule out strain-specific effects. We conclude that post-meiotic germ cells, specifically the spermatids or sperm that are lacking from *brca2* mutants, control growth of surrounding somatic cells by an as yet unknown mechanism that is secondary to *brca2*-impaired spermatogenesis.

The Animal Pole Distribution of *brca2* Transcript Does Not Appear to Generate Oocyte Polarity

Our gene expression analyses showed unexpectedly that *brca2* transcript localizes asymmetrically at the animal pole of wild-type oocytes. The asymmetrical distribution of certain mRNAs in the oocyte cytoplasm helps to promote animal or vegetal pole identity [41,42,60-62]. In *brca2;tp53* double mutants, however, the localization of messages for *pou5f1*, *vasa*, and even *brca2* itself were normal, suggesting that *brca2* activity is not essential to polarize the oocyte cytoplasm. Furthermore, *brca2* transcript begins to be localized in stage III oocytes but *ccnb1* transcripts begin to be localized earlier [41,42], a timing that is incompatible with the hypothesis that *brca2* initiates ooplasm asymmetry. The germinal vesicle (the oocyte nucleus) lies in the center of stage I-III oocytes, but moves to the animal pole by stage IV [41,49]; thus, the oocyte nucleus -- and hence the resulting zygote and cleavage nuclei -- occupy cytoplasm enriched in *brca2* transcript. The translation of this transcript would be available to support the repair of DNA damage incurred in the rapid divisions of cleavage before zygotic transcription initiates at the mid-blastula transition. The observation that *brca2*;*tp53* double mutant females formed doubly heterozygous embryos that cleaved normally, completed gastrulation, but then died by 24 hpf supports the notion that maternally transmitted *brca2* transcript is important for normal early development and that zygotic *brca2* transcript is too little or too late to rescue the phenotype.

Brca2 Activity Is Essential for Normal Architecture of the Oocyte Nucleus

brca2;tp53 double mutant females produced oocytes with normally organized ooplasm but aberrantly organized nuclei. Developing oocytes that lacked *brca2* activity partitioned nucleoli aberrantly to one side of the nucleus rather than their usual radial location and distributed chromosomes opposite to the nucleoli rather than their normal central position. Although these ovaries were also homozygous mutant for *tp53* (which was necessary to obtain homozygous *brca2* mutant females), the oocyte nucleus architecture defect is due to *brca2* deficiency because homozygous *tp53* mutant females form normal oocytes [58,59], as we confirmed. Oocytes in *brca2;tp53* females reached the bouquet stage of meiosis in which telomeres cluster at one side of the oocyte. The asymmetric localization of chromosomes in the oocytes of *brca2;tp53* females may result from a deficiency in DNA repair that inhibits exit from the bouquet stage. This could result, for example, if Brca2 is necessary for the relaxation of telomere clustering that generates the bouquet stage, a proposition supported by the high rate of recombination in subtelomeric sequences [81]: a high rate of recombination near the telomeres could create interlinked chromosomes like the radial reunion figures we observed in somatic cell chromosomes and these links might not permit normal chromosome dispersal in the nucleoplasm. It is unclear, however, how the abnormal persistence of chromosome clustering would generate the asymmetric distribution and abnormal morphologies of nucleoli that we found in oocytes of mutant females. *Drosophila brca2* mutants develop oocytes with an abnormally asymmetric karyosome and dorsoventral defects [46], phenotypes that may be functionally related to those we observe in zebrafish. Transgenic female mice rescued with a human *BRCA2*-containing BAC have abnormal polar bodies in meiosis [24], a phenotype that may be a consequence of nuclear symmetry problems we demonstrate here in zebrafish. We conclude that *brca2* is generally important for the organization of oocyte nuclei both in protostomes and in vertebrates.

brca2;tp53 Double Mutant Females and Invasive Ovarian Tumors

Tp53 deficiency coupled with diminished Brca2 activity promotes mammalian breast tumors [8]. Likewise, zebrafish *brca2*;*tp53* double mutants develop invasive ovarian tumors, and these appear earlier and more frequently than tumors in animals with lower Tp53 activity alone. We conclude that zebrafish shares with human and rat [10] a requirement for Brca2 activity to help suppress the formation of ovarian cancers. The genome instability we observed in *brca2* mutant tissue culture cells may contribute to tumor formation because zebrafish *gin* mutations identified on the basis of genomic instability have elevated cancer risk [82]. Future studies are necessary to better understand the etiology of *brca2*-dependent ovarian tumors in zebrafish.

FANCD1 is an alias of *BRCA2* because homozygous hypomorphic mutations in this gene cause Fanconi Anemia while heterozygous null mutations increase the risk of breast and ovarian tumors and homozygous null mutations cause lethality [11]. In addition to genome instability, bone marrow failure, leukemia, and squamous cell carcinomas, many FA patients experience hypogonadism, impaired gametogenesis, defective meiosis, and sterility [19,83]. Thus, zebrafish *brca2*(*fancd1*) shares genome instability and gonad developmental phenotypes with FA

patients and ovarian tumors with human heterozygotes for *BRCA2* mutations. These findings indicate that zebrafish *brca2* mutants provide a suitable model for human *BRCA2*-related disease. In a result of special significance, the embryonic sensitivity of zebrafish *brca2* mutants to a DNA damage agent provides an assay for a small molecule screen to identify compounds that can rescue the DNA damage phenotype and thus has the potential to contribute to the discovery of substances that can ameliorate at least some of the phenotypes observed in human patients.

Methods

DNA Amplification and Cloning

A partial gene model for zebrafish *brca2* was inferred using GenomeScan (http://genes.mit.edu/genomescan.html) to match the human BRCA2 protein to a zebrafish genomic BAC clone we identified and sequenced (Genbank accession #AC149226). Primers for RACE (Clontech) were designed using this preliminary gene model. RACE template was 5′ first-strand zebrafish cDNA synthesized from pooled mRNA from embryos at 12, 24, and 48 hours post-fertilization (hpf). A BLAST search of the zebrafish EST database (http://www.ncbi.nlm.nih.gov/genome/seq/BlastGen/BlastGen.cgi?taxid = 7955) using the 3′ UTR modeled with GenomeScan recovered EST CT605096. This EST and our GenomeScan model were used to design primers for amplification of the entire *brca2* cDNA (primers in Table S1) using as template second strand cDNA from 60hpf embryos. Amplified fragments were cloned using the TOPO Cloning Kit for Sequencing (Invitrogen).

Bioinformatics

We applied reciprocal best BLAST "hit" (RBH) [84] as an initial test for orthology of zebrafish and human *BRCA2* genes. We queried the stickleback genome (http://www.ensembl.org/Gasterosteus_aculeatus/blastview) using zebrafish Brca2 and found stickleback *brca2* on contig 2939. This contig, together with human BRCA2, was used to develop a preliminary gene model for stickleback *brca2* (Figure S1). The Synteny Database identified paralogous and orthologous chromosome segments [26].

Animals

The insertional *brca2* mutant (ZM_00075660) was purchased from Znomics, which randomly inserted derivatives of a Moloney murine leukemia-based retroviral vector into zebrafish [85]. To genotype ZM_00075660, we used primers F4/R4 to amplify the mutant allele, and primers F1/R1 to amplify the wild-type allele. Table S1 lists primer sequences. To reduce Tp53 activity, the hypomorphic mutation *tp53*^{M214K} was obtained from ZIRC (http://zebrafish.org/zirc/home/guide.php) and was used and genotyped as described [58]. All animals were reared and collected under standard conditions [86]. The University of Oregon Institutional Animal Care and Use Committee approved all animal work (Animal Welfare Assurance Number A-3009-01, IACUC protocol #08-13). Genetic nomenclature follows guidelines from ZFIN (http://zfin.org/zf_info/nomen.html), e.g., human gene, *BRCA2*; mouse gene, *Brca2;* zebrafish gene, *brca2;* human protein BRCA2 and mouse and zebrafish protein, Brca2.

In Situ Hybridization and Histology

Whole mount *in situ* hybridizations were performed as described [87] using several individuals for each developmental stage. *In situ* hybridization experiments on zebrafish cryosections were performed following [52]. Probes for *amh and cyp19a1a* were made following [52] and probe for *vasa* was made from its 3′end as described [51]. A *brca2* cDNA fragment of 725nt (nucleotides 2627-3351 of NM_001110394), a *pou5f1* cDNA fragment of 778nt (nucleotides 705-1482 of NM_131112), and a *sycp3* cDNA fragment of 620nt (nucleotides 265-884 of NM_001040350) were used to synthesize DIG-labeled riboprobe (Boehringer Mannheim). For gonad histology, paraffin embedded Bouin's fixed tissue was sectioned at 7 microns and stained with hematoxylin and eosin.

Immunohistochemistry

Animals were fixed at 60dpf in 4% PFA overnight at 4°C, embedded in paraffin, and sectioned at 7 microns. Apoptotic cells were detected by immunofluorescence using anti-active Caspase-3 (Pharmingen, # 559565 Purified Rabbit anti-active caspase-3) following published protocols [20,39].

dead end Morpholino Injections

Animals depleted of germ cells were obtained by injecting wild-type zebrafish embryos from the AB strain at the 1–2 cell stage with *dead end* antisense morpholino oligonucleotide (Gene Tools) as described [88]. Injected and non-injected animals were raised to adulthood and collected at 18 months post-fertilization.

Acridine Orange Staining

Embryos were exposed to diepoxybutane (DEB) in embryo medium from 7–28hpf, or left untreated. Embryos were stained with acridine orange (AO) and mounted following [89]. The initial focal plane was the otolith, and a z-series consisting of seven 10-micron steps was captured on a Bio-Rad Radiance 2100 confocal microscope. Images were merged into a single plane with Velocity 4.4.0 and the number of AO-positive cells in the central nervous system anterior to the beginning of the yolk extension was quantified using ImageJ.

Karyotyping

Distal tips of caudal and dorsal fins from mutant and wild-type adult fish were cultured in 1:1 (vol/vol) DMEM (Gibco) and Amniopan (PAN) media supplemented with 100 µg/ml penicillin and 0.1 mg/ml streptomycin in a 5% CO2 atmosphere at 28°C. Adherent fibroblast-like cells grew from primary explants. When culture flasks were confluent, cells were trypsinized and subcultured at split ratios of 1:4. Cells of the 20th or 21st passage were exposed to 5 or 10 ng/ml mitomycin C for 24 hrs and screened for chromosome morphology. Rates of chromatid and chromosome breaks, radial reunion figures, and other categories of breakage were scored by analyzing 100 cells from each cell line. To visualize mitotic chromosomes, subconfluent cultures were exposed to colcemid for 3 hrs. Accumulated metaphases were prepared following standard methods. Slides were stained with 5% Giemsa solution. Metaphases were screened under a light microscope. Line authenticity was confirmed by PCR genotyping using the primer set Brca2zmwt.F2 5′-GCAGGTTGTGATGAAGCCACC-3′ and Brca2zmwt.R1 5′-GTGGTGTGAGGCCAGAGGTT-3′ for amplification of a 888-bp fragment of the wt *brca2* sequence and the primer set 5Fd1ins.F 5′-CTTGCGCACCAAGGCTTCAC-3′ and 5Fd1ins.R 5′-ACCGCATCTGGGGACCATCT-3′ for amplification of a 971-bp fragment of the insert. For cell growth studies, 1×10^5 cells per line were seeded into six flasks. Following trypsinization, one flask per line was counted daily until day 5. Resulting numbers were plotted as multiples of the initial cell count. Mitomycin C (MMC) was added at given concentrations at time 0 h. For flow cytometric assays, cultures were harvested and cells were washed twice with PBS and

fixed in 4% paraformaldehyde at 37°C for 10 min. The reaction was stopped on ice for 2 min, then cells were pelleted and resuspended in 100% methanol at −20°C for permeabilization. For immunostaining, we used the CaspGLOW Fluorescein Active Caspase-3 Staining Kit (BioVision # K183-25) and propidium iodide (PI) counterstain at a final concentration of 8 µg/ml. Histograms were recorded on an analytical, triple-laser equipped flow cytometer (LSRII, Becton Dickinson) using Sapphire 488 nm solid state laser excitation of 5(6)-fluorescein isothiocyanate (FITC) and propidium iodide (PI) with appropriate filter sets to discern fluorescence intensity of different emission wavelengths. Quantification of cell distributions was by FACSDiva Software, version 6.1.

Supporting Information

Figure S1 Sequence of Brca2 inferred from the well-assembled sequenced genome of the stickleback, *Gasterosteus aculeatus*. The stickleback sequence was used as a comparator to infer the structure of the zebrafish *brca2* gene. Ensembl (http://www.ensembl.org/Gasterosteus_aculeatus/blastview) was searched using as query *brca2* exons conserved between zebrafish and human. This search recovered stickleback contig 2939, the sequence of which allowed the construction of a preliminary model for stickleback *brca2* by comparing contig 2939 to human *BRCA2*. This comparison allowed us to clarify zebrafish BRC repeats.
Found at: doi:10.1371/journal.pgen.1001357.s001 (1.14 MB TIF)

Figure S2 Analysis of zebrafish BRC repeats. (A) Alignment of the eight mammalian BRC repeats to the corresponding repeats in zebrafish and stickleback. Sequence identity between homologous zebrafish and human BRC repeats varied from 16% (BRC1) to 50% (BRC7) (mean = 38%). (B) Alignment of zebrafish BRC repeats identified four more (w,x,y,z) than are found in mammalian Brca2 proteins. A pairwise comparison of the 12 zebrafish BRC repeats to each other showed sequence identities between 19% and 96%.
Found at: doi:10.1371/journal.pgen.1001357.s002 (0.81 MB TIF)

Figure S3 Sequence of the DNA binding domain (DBD) of Brca2 in four vertebrates, zebrafish, human chicken, and mouse. Abbreviations: HD, helical domain; OB, oligo nucleotide binding motifs.
Found at: doi:10.1371/journal.pgen.1001357.s003 (1.22 MB TIF)

Figure S4 Expression of *brca2* during zebrafish development. (A) Expression of brca2 during zebrafish development assayed by RT-PCR. Total RNA was extracted using TRI REAGENT according to manufacturer's instructions (Molecular Research Center Inc., TR-118) from pools of 40 to 50 embryos for each developmental stage. First strand cDNA was generated from 2 µg of total RNA using Superscript III Rnase H-reverse transcriptase (Invitrogen, #18080-044) and oligo(dT) primer. Reverse transcriptase was deactivated by incubating the sample at 70°C for 15 minutes, followed by RNA digestion with RNase H (New England Biolabs, M0297S). A dilution 1:20 of the first strand cDNA was used to assay *brca2* gene expression by non-quantitative PCR using the gene specific oligonucleotides 5′-GGGCCAGAAAACACAG-CAACTCAAA-3′ and 5′-GCACAGGCCCAGATAG-CACTCG-3′. Detection of actin expression (oligonucleotides: 5′-GAGAAGATCTGGCATCACACCTTC-3′ and 5′-GGTCTGTGGATACCGCAAGATTC-3′) was used as an internal control. Results showed substantial *brca2* transcript in early (1–2 cells) and later cleavage stages, demonstrating maternal transcript, which apparently was supplemented from the beginning of zygotic transcription until at least 5dpf. (B–E) Whole mount *in situ* hybridization to embryos at 1, 12, 24, and 48 hpf shows maternal expression, broad low level expression, and higher expression in rapidly dividing cells. (F–K) *In situ* hybridization to sections at the ages indicated shows expression in the central nervous system (cns) and in the spinal cord (sc). (L) Expression in the adult brain (sagittal section at position in L′) continued in proliferative zones. (M) The adult kidney expressed *brca2* strongly in the hematopoietic marrow. (N) The adult intestine (cross section) expressed more strongly in proliferative centers. Abbreviations: cce, cerebellar corpus; cns, central nervous system; eg, granular eminence; epi, epiboly; in, intervillus region; ma, kidney marrow; Neg. ctrl, negative control; ob, olfactory bulb; pg, preglomerular area; pgz, periventricular gray zone of optic tectum; pa, pharyngeal arches; r, retina; sl, spinal cord; som, somites; teo, optic tectum; tel, telencephalon; tev, tectal ventricle; tu, kidney tubules; val, lateral division of valvula cerebelli.
Found at: doi:10.1371/journal.pgen.1001357.s004 (6.54 MB TIF)

Figure S5 *brca2* mutant embryos exhibited normal hematopoietic development. Human Fanconi anemia patients develop profound anemia of several lineages. To investigate hematopoietic development in zebrafish *brca2*(*fancd1*) mutants, we studied gene expression patterns. Results showed that 16-somite stage wild-type embryos (A) and mutant (B) embryos had the same expression pattern for the early hematopoietic marker *scl* (A, B) and the 'master hematopoietic' gene *lmo2* (wild type, C, mutant, D). Furthermore, 24 hpf embryos had normal expression of *pu.1*, a marker of myeloid progenitors (E, F), *mpo* a marker of primitive myelopoiesis (G, H), and *gata1*, a marker of erythropoietic development (I,J). Late stage hematopoietic markers were also expressed normally in *brca2* mutants, including the myelopoietic gene *mpo* (K,L), the leukocyte gene *l-plastin* (M,N), and the erythrocyte gene α*-globin* (O,P) in 2dpf embryos, and *myb* (Q,R) in 3dpf embryos in definitive hematopoiesis. In addition, expression of the T-lymphocyte gene *rag1* was normal in 5dpf embryos (S,T). We conclude that, in contrast to humans but more similar to mouse, embryonic hematopoietic development appears to be normal in *brca2*(*fancd1*) mutants.
Found at: doi:10.1371/journal.pgen.1001357.s005 (5.43 MB TIF)

Figure S6 Expression of female-specific, male-specific, and meiotic recombination markers in adjacent sections of 47dpf wild-type and *brca2* mutant gonads revealed male development in *brca2* immature mutant testis. Oocytes in wild-type ovaries strongly expressed *vasa* (A) and weakly expressed *amh* in granulosa cells (B). Somatic cells of the ovary expressed *cyp19a1a* (C), but at this stage, expression of the meiotic marker *sycp3* was weak in the ovary (D). Wild-type testes expressed *vasa* in early germ cells (E) and *amh* in well-organized Sertoli cells surrounding testis tubules (F), but not *cyp19a1a* (G). (H) Spermatocytes expressed *sycp3* in wild type testes. (I–L) In contrast, *brca2* mutant testes showed hypogonadism but contained *vasa*-expressing cells (I), disorganized and fewer Sertoli cells expressing *amh* (J), and no expression of the female marker *cyp19a1a* (K), but spermatocytes did express the recombination meiotic marker *sycp3* (L). Arrows point out examples of regions of expression.
Found at: doi:10.1371/journal.pgen.1001357.s006 (7.37 MB TIF)

Figure S7 Brca2 function is not essential to localize *brca2*, *pou5f1*, or *vasa* transcripts in zebrafish oocytes. (A–F) *In situ* hybridizations on serial sections of wild-type (A–C) and *brca2;tp53* double mutant females (D–F). In wild-type ovaries transcripts of the *brca2* (A) and *pou5f1* (B) genes localized to the same small cortical region of stage III oocytes while *vasa* transcripts localized to the opposite pole of the same individual oocytes (C). Similarly, serial sections of ovaries

from *brca2;tp53* double mutants showed the same tight localization of *brca2* (D) and *pou5f1* (E) transcripts to one pole and *vasa* transcripts to the other pole (F). We conclude that *brca2* function is not essential to define polarity of the oocyte cytoplasm. Red arrowheads: animal pole markers; green dotted line: vegetal pole expression.
Found at: doi:10.1371/journal.pgen.1001357.s007 (8.21 MB TIF)

Table S1 Primers for *brca2(fancd1)* RACE-PCR, PCR, genotyping, and cDNA analysis. Numbers correspond to the position of the most 3′ base on the *Danio* cDNA sequence (Accession number NM_001110394.1). Primers F1-F4 and R1-R4 correspond to those in Figure 3.
Found at: doi:10.1371/journal.pgen.1001357.s008 (0.06 MB DOC)

Acknowledgments

We thank Wenbiao Chen, Greg Golling, and Roger Cone of Znomics for the insertional mutation in *brca2*; ZIRC for providing the *tp53* zebrafish mutant line; P. K. Loi, N. Banning, and B. Wiskow from the University of Oregon Histology Facility for sample sectioning; and A. Rapp, M. McFadden, R. Montgomery, T. Mason, and the University of Oregon Zebrafish Facility for providing fish care.

Author Contributions

Conceived and designed the experiments: ARM CW TAT IN DS JHP. Performed the experiments: ARM CW TAT CC RAB YLY IN AJ EMG XH DS JHP. Analyzed the data: ARM CW TAT CC RAB YLY JPK JS DS JHP. Contributed reagents/materials/analysis tools: ARM CW TAT. Wrote the paper: ARM CW TAT CC IN DS JHP.

References

1. Wooster R, Weber BL (2003) Breast and ovarian cancer. N Engl J Med 348: 2339–2347.
2. Edwards SM, Kote-Jarai Z, Meitz J, Hamoudi R, Hope Q, et al. (2003) Two percent of men with early-onset prostate cancer harbor germline mutations in the BRCA2 gene. Am J Hum Genet 72: 1–12.
3. Gayther SA, de Foy KA, Harrington P, Pharoah P, Dunsmuir WD, et al. (2000) The frequency of germ-line mutations in the breast cancer predisposition genes BRCA1 and BRCA2 in familial prostate cancer. The Cancer Research Campaign/British Prostate Group United Kingdom Familial Prostate Cancer Study Collaborators. Cancer Res 60: 4513–4518.
4. Easton D (1997) Breast cancer genes--what are the real risks? Nat Genet 16: 210–211.
5. Antoniou A, Pharoah PD, Narod S, Risch HA, Eyfjord JE, et al. (2003) Average risks of breast and ovarian cancer associated with BRCA1 or BRCA2 mutations detected in case Series unselected for family history: a combined analysis of 22 studies. Am J Hum Genet 72: 1117–1130.
6. Tavtigian SV, Simard J, Rommens J, Couch F, Shattuck-Eidens D, et al. (1996) The complete BRCA2 gene and mutations in chromosome 13q-linked kindreds. Nat Genet 12: 333–337.
7. Connor F, Smith A, Wooster R, Stratton M, Dixon A, et al. (1997) Cloning, chromosomal mapping and expression pattern of the mouse Brca2 gene. Hum Mol Genet 6: 291–300.
8. Moynahan ME (2002) The cancer connection: BRCA1 and BRCA2 tumor suppression in mice and humans. Oncogene 21: 8994–9007.
9. Frappart PO, McKinnon PJ (2007) BRCA2 function and the central nervous system. Cell Cycle 6: 2453–2457.
10. Cotroneo MS, Haag JD, Zan Y, Lopez CC, Thuwajit P, et al. (2007) Characterizing a rat Brca2 knockout model. Oncogene 26: 1626–1635.
11. Neveling K, Endt D, Hoehn H, Schindler D (2009) Genotype-phenotype correlations in Fanconi anemia. Mutat Res 668: 73–91.
12. D'Andrea A (2003) Fanconi anemia. Curr Biol 13: R546.
13. Bagby GC, Alter BP (2006) Fanconi anemia. Semin Hematol 43: 147–156.
14. Rosenberg PS, Alter BP, Ebell W (2008) Cancer risks in Fanconi anemia: findings from the German Fanconi Anemia Registry. Haematologica 93: 511–517.
15. Howlett NG, Taniguchi T, Olson S, Cox B, Waisfisz Q, et al. (2002) Biallelic inactivation of BRCA2 in Fanconi anemia. Science 297: 606–609.
16. Hirsch B, Shimamura A, Moreau L, Baldinger S, Hag-alshiekh M, et al. (2004) Association of biallelic BRCA2/FANCD1 mutations with spontaneous chromosomal instability and solid tumors of childhood. Blood 103: 2554–2559.
17. Alter BP, Rosenberg PS, Brody LC (2007) Clinical and molecular features associated with biallelic mutations in FANCD1/BRCA2. J Med Genet 44: 1–9.
18. Moynahan ME, Cui TY, Jasin M (2001) Homology-directed dna repair, mitomycin-c resistance, and chromosome stability is restored with correction of a Brca1 mutation. Cancer Res 61: 4842–4850.
19. Wong JC, Alon N, McKerlie C, Huang JR, Meyn MS, et al. (2003) Targeted disruption of exons 1 to 6 of the Fanconi Anemia group A gene leads to growth retardation, strain-specific microphthalmia, meiotic defects and primordial germ cell hypoplasia. Hum Mol Genet 12: 2063–2076.
20. Rodríguez-Marí A, Cañestro C, BreMiller RA, Nguyen-Johnson A, Asakawa K, et al. (2010) Sex Reversal in Zebrafish fancl Mutants Results from Tp53-Mediated Germ Cell Apoptosis. PLoS Genet 6: e1001034.
21. Li X, Le Beau MM, Ciccone S, Yang FC, Freie B, et al. (2005) Ex vivo culture of Fancc−/− stem/progenitor cells predisposes cells to undergo apoptosis, and surviving stem/progenitor cells display cytogenetic abnormalities and an increased risk of malignancy. Blood 105: 3465–3471.
22. Chen PL, Chen CF, Chen Y, Xiao J, Sharp ZD, et al. (1998) The BRC repeats in BRCA2 are critical for RAD51 binding and resistance to methyl methanesulfonate treatment. Proc Natl Acad Sci U S A 95: 5287–5292.
23. Hakem R, de la Pompa JL, Mak TW (1998) Developmental studies of Brca1 and Brca2 knock-out mice. J Mammary Gland Biol Neoplasia 3: 431–445.
24. Sharan SK, Pyle A, Coppola V, Babus J, Swaminathan S, et al. (2004) BRCA2 deficiency in mice leads to meiotic impairment and infertility. Development 131: 131–142.
25. Titus TA, Yan YL, Wilson C, Starks AM, Frohnmayer JD, et al. (2009) The Fanconi anemia/BRCA gene network in zebrafish: embryonic expression and comparative genomics. Mutat Res 668: 117–132.
26. Catchen JM, Conery JS, Postlethwait JH (2009) Automated identification of conserved synteny after whole-genome duplication. Genome Res 19: 1497–1505.
27. Postlethwait JH, Woods IG, Ngo-Hazelett P, Yan Y-L, Kelly PD, et al. (2000) Zebrafish comparative genomics and the origins of vertebrate chromosomes. Genome Res 10: 1890–1902.
28. Titus TA, Selvig DR, Qin B, Wilson C, Starks AM, et al. (2006) The Fanconi anemia gene network is conserved from zebrafish to human. Gene 371: 211–223.
29. Amores A, Force A, Yan Y-L, Joly L, Amemiya C, et al. (1998) Zebrafish *hox* clusters and vertebrate genome evolution. Science 282: 1711–1714.
30. Taylor J, Braasch I, Frickey T, Meyer A, Van De Peer Y (2003) Genome duplication, a trait shared by 22,000 species of ray-finned fish. Genome Res 13: 382–390.
31. Jaillon O, Aury JM, Brunet F, Petit JL, Stange-Thomann N, et al. (2004) Genome duplication in the teleost fish Tetraodon nigroviridis reveals the early vertebrate proto-karyotype. Nature 431: 946–957.
32. Teng DH, Bogden R, Mitchell J, Baumgard M, Bell R, et al. (1996) Low incidence of BRCA2 mutations in breast carcinoma and other cancers. Nat Genet 13: 241–244.
33. Takata M, Tachiiri S, Fujimori A, Thompson LH, Miki Y, et al. (2002) Conserved domains in the chicken homologue of BRCA2. Oncogene 21: 1130–1134.
34. Warren M, Smith A, Partridge N, Masabanda J, Griffin D, et al. (2002) Structural analysis of the chicken BRCA2 gene facilitates identification of functional domains and disease causing mutations. Hum Mol Genet 11: 841–851.
35. Milner J (1997) Structures and functions of the tumor suppressor p53. Pathol Biol (Paris) 45: 797–803.
36. Bignell G, Micklem G, Stratton MR, Ashworth A, Wooster R (1997) The BRC repeats are conserved in mammalian BRCA2 proteins. Hum Mol Genet 6: 53–58.
37. Yang H, Jeffrey PD, Miller J, Kinnucan E, Sun Y, et al. (2002) BRCA2 function in DNA binding and recombination from a BRCA2-DSS1-ssDNA structure. Science 297: 1837–1848.
38. Deutsch M, Long M (1999) Intron-exon structures of eukaryotic model organisms. Nucleic Acids Res 27: 3219–3228.
39. Cheesman SE, Neal JT, Mittge E, Seredick BM, Guillemin K (2010) Microbes and Health Sackler Colloquium: Epithelial cell proliferation in the developing zebrafish intestine is regulated by the Wnt pathway and microbial signaling via Myd88. Proc Natl Acad Sci U S A.
40. Zabludoff SD, Wright WW, Harshman K, Wold BJ (1996) BRCA1 mRNA is expressed highly during meiosis and spermiogenesis but not during mitosis of male germ cells. Oncogene 13: 649–653.
41. Howley C, Ho RK (2000) mRNA localization patterns in zebrafish oocytes. Mech Dev 92: 305–309.
42. Abrams EW, Mullins MC (2009) Early zebrafish development: it's in the maternal genes. Curr Opin Genet Dev 19: 396–403.
43. Schroeder TM, Anschutz F, Knopp A (1964) Spontane Chromosomenaberrationen bei familiärer Panmyelopathie. Humangenetik 1: 194–196.
44. Auerbach AD (1993) Fanconi anemia diagnosis and the diepoxybutane (DEB) test. Exp Hematol 21: 731–733.
45. Darzynkiewicz Z (1990) Differential staining of DNA and RNA in intact cells and isolated cell nuclei with acridine orange. Methods Cell Biol 33: 285–298.

46. Klovstad M, Abdu U, Schupbach T (2008) Drosophila brca2 is required for mitotic and meiotic DNA repair and efficient activation of the meiotic recombination checkpoint. PLoS Genet 4: e31.
47. Takahashi H (1977) Juvenile hermaphroditism in the zebrafish, Brachydanio rerio. Bull Fac Fish Hokkaido Univ 28: 57–65.
48. Uchida D, Yamashita M, Kitano T, Iguchi T (2002) Oocyte apoptosis during the transition from ovary-like tissue to testes during sex differentiation of juvenile zebrafish. J Exp Biol 205: 711–718.
49. Selman K, Wallace RA, Sarka A, Q. X (1993) Stages of oocyte development in the zebrafish Brachydanio rerio. J Morphol 218: 203–224.
50. Dai C, Krantz SB (1999) Interferon gamma induces upregulation and activation of caspases 1, 3, and 8 to produce apoptosis in human erythroid progenitor cells. Blood 93: 3309–3316.
51. Yoon C, Kawakami K, Hopkins N (1997) Zebrafish vasa homologue RNA is localized to the cleavage planes of 2- and 4-cell-stage embryos and is expressed in the primordial germ cells. Development 124: 3157–3165.
52. Rodriguez-Mari A, Yan YL, Bremiller RA, Wilson C, Canestro C, et al. (2005) Characterization and expression pattern of zebrafish Anti-Mullerian hormone (Amh) relative to sox9a, sox9b, and cyp19a1a, during gonad development. Gene Expr Patterns 5: 655–667.
53. von Hofsten J, Larsson A, Olsson PE (2005) Novel steroidogenic factor-1 homolog (ff1d) is coexpressed with anti-Mullerian hormone (AMH) in zebrafish. Dev Dyn 233: 595–604.
54. Chiang EF, Yan YL, Guiguen Y, Postlethwait J, Chung B (2001) Two Cyp19 (P450 aromatase) genes on duplicated zebrafish chromosomes are expressed in ovary or brain. Mol Biol Evol 18: 542–550.
55. Moens PB (2006) Zebrafish: chiasmata and interference. Genome 49: 205–208.
56. Zickler D, Kleckner N (1998) The leptotene-zygotene transition of meiosis. Annu Rev Genet 32: 619–697.
57. Scherthan H (2001) A bouquet makes ends meet. Nat Rev Mol Cell Biol 2: 621–627.
58. Berghmans S, Murphey RD, Wienholds E, Neuberg D, Kutok JL, et al. (2005) tp53 mutant zebrafish develop malignant peripheral nerve sheath tumors. Proc Natl Acad Sci U S A 102: 407–412.
59. Parant JM, George SA, Holden JA, Yost HJ (2010) Genetic modeling of Li-Fraumeni syndrome in zebrafish. Dis Model Mech 3: 45–56.
60. Kosaka K, Kawakami K, Sakamoto H, Inoue K (2007) Spatiotemporal localization of germ plasm RNAs during zebrafish oogenesis. Mech Dev 124: 279–289.
61. Marlow FL, Mullins MC (2008) Bucky ball functions in Balbiani body assembly and animal-vegetal polarity in the oocyte and follicle cell layer in zebrafish. Dev Biol 321: 40–50.
62. Lindeman RE, Pelegri F (2010) Vertebrate maternal-effect genes: Insights into fertilization, early cleavage divisions, and germ cell determinant localization from studies in the zebrafish. Mol Reprod Dev 77: 299–313.
63. Leal MC, Cardoso ER, Nobrega RH, Batlouni SR, Bogerd J, et al. (2009) Histological and stereological evaluation of zebrafish (Danio rerio) spermatogenesis with an emphasis on spermatogonial generations. Biol Reprod 81: 177–187.
64. Slanchev K, Stebler J, de la Cueva-Mendez G, Raz E (2005) Development without germ cells: the role of the germ line in zebrafish sex differentiation. Proc Natl Acad Sci U S A 102: 4074–4079.
65. Youngren KK, Coveney D, Peng X, Bhattacharya C, Schmidt LS, et al. (2005) The Ter mutation in the dead end gene causes germ cell loss and testicular germ cell tumours. Nature 435: 360–364.
66. Sharan SK, Morimatsu M, Albrecht U, Lim DS, Regel E, et al. (1997) Embryonic lethality and radiation hypersensitivity mediated by Rad51 in mice lacking Brca2. Nature 386: 804–810.
67. Force A, Lynch M, Pickett FB, Amores A, Yan Y-L, et al. (1999) Preservation of duplicate genes by complementary, degenerative mutations. Genetics 151: 1531–1545.
68. Hussain S, Wilson JB, Medhurst AL, Hejna J, Witt E, et al. (2004) Direct interaction of FANCD2 with BRCA2 in DNA damage response pathways. Hum Mol Genet 13: 1241–1248.
69. Kane DA, Kimmel CB (1993) The zebrafish midblastula transition. Development 119: 447–456.
70. Auerbach AD, Wolman SR (1976) Susceptibility of Fanconi's anaemia fibroblasts to chromosome damage by carcinogens. Nature 261: 494–496.
71. Houghtaling S, Newell A, Akkari Y, Taniguchi T, Olson S, et al. (2005) Fancd2 functions in a double strand break repair pathway that is distinct from non-homologous end joining. Hum Mol Genet 14: 3027–3033.
72. Domchek SM, Merillat SL, Tigges J, Tweed AJ, Weinar M, et al. (2005) Sex ratio skewing of offspring in families with hereditary susceptibility to breast cancer. J Med Genet 42: 511–513.
73. Moldovan GL, D'Andrea AD (2009) How the fanconi anemia pathway guards the genome. Annu Rev Genet 43: 223–249.
74. Godthelp BC, Wiegant WW, Waisfisz Q, Medhurst AL, Arwert F, et al. (2006) Inducibility of nuclear Rad51 foci after DNA damage distinguishes all Fanconi anemia complementation groups from D1/BRCA2. Mutat Res 594: 39–48.
75. Tarsounas M, Davies D, West SC (2003) BRCA2-dependent and independent formation of RAD51 nuclear foci. Oncogene 22: 1115–1123.
76. Maack G, Segner H (2003) Morphological development of the gonads in zebrafish. J Fish Biol 62: 895–906.
77. Wang X, Bartfai R, Sleptsova-Freidrich I, Orban L (2007) The timing and extent of 'juvenile ovary' phase are highly variable during zebrafish testis differentiation. Journal of Fish Biology 70: 33–44.
78. Siegfried KR, Nusslein-Volhard C (2008) Germ line control of female sex determination in zebrafish. Dev Biol.
79. Draper BW, McCallum CM, Moens CB (2007) nanos1 is required to maintain oocyte production in adult zebrafish. Dev Biol 305: 589–598.
80. Houwing S, Kamminga LM, Berezikov E, Cronembold D, Girard A, et al. (2007) A role for Piwi and piRNAs in germ cell maintenance and transposon silencing in Zebrafish. Cell 129: 69–82.
81. Paigen Kea (2008) The recombinational anatomy of a mouse chromosome. PLoS Genet 4: e1000119.
82. Moore JL, Rush LM, Breneman C, Mohideen MA, Cheng KC (2006) Zebrafish genomic instability mutants and cancer susceptibility. Genetics 174: 585–600.
83. Auerbach AD (2009) Fanconi anemia and its diagnosis. Mutat Res 668: 4–10.
84. Hirsh AE, Fraser HB (2001) Protein dispensability and rate of evolution. Nature 411: 1046–1049.
85. Amsterdam A, Hopkins N (2006) Mutagenesis strategies in zebrafish for identifying genes involved in development and disease. Trends Genet 22: 473–478.
86. Westerfield M (1995) The zebrafish book: a guide for the laboratory use of zebrafish (*Danio rerio)*. Eugene, OR: University of Oregon Press.
87. Yan YL, Miller CT, Nissen R, Singer A, Liu D, et al. (2002) A zebrafish sox9 gene required for cartilage morphogenesis. Development 129: 5065–5079.
88. Weidinger G, Stebler J, Slanchev K, Dumstrei K, Wise C, et al. (2003) dead end, a novel vertebrate germ plasm component, is required for zebrafish primordial germ cell migration and survival. Curr Biol 13: 1429–1434.
89. Reimers MJ, La Du JK, Periera CB, Giovanini J, Tanguay RL (2006) Ethanol-dependent toxicity in zebrafish is partially attenuated by antioxidants. Neurotoxicol Teratol 28: 497–508.
90. Higgins DG, Sharp PM (1988) CLUSTAL: a package for performing multiple sequence alignment on a microcomputer. Gene 73: 237–244.
91. Perriere G, Gouy M (1996) WWW-query: an on-line retrieval system for biological sequence banks. Biochimie 78: 364–369.
92. Kyte J, Doolittle RF (1982) A simple method for displaying the hydropathic character of a protein. J Mol Biol 157: 105–132.